



**CHALMERS**  
UNIVERSITY OF TECHNOLOGY



# **Wind power with hydrogen production, storage, and reconversion as flexible baseload in the Nordic energy system**

Master's thesis in Sustainable Energy Systems

**QUINN SARAH HANITIO**  
**MARÍA ZAS BUSTINGORRI**

---

**DEPARTMENT OF SPACE, EARTH AND ENVIRONMENT**

**CHALMERS UNIVERSITY OF TECHNOLOGY**

Gothenburg, Sweden 2023

[www.chalmers.se](http://www.chalmers.se)



MASTER'S THESIS 2023

Wind power with hydrogen production, storage,  
and reconversion as flexible baseload in the  
Nordic energy system

Quinn Sarah Hanitio  
María Zas Bustingorri



Department of Space, Earth and Environment  
*Division of Energy Technology*  
Energy Systems  
CHALMERS UNIVERSITY OF TECHNOLOGY  
Gothenburg, Sweden 2023

Wind power with hydrogen production, storage, and reconversion as flexible baseload  
in the Nordic energy system

© QUINN SARAH HANITIO, MARÍA ZAS BUSTINGORRI, 2023.

Supervisor: Simon Öberg, Space, Earth and Environment  
Examiner: Filip Johnsson, Space, Earth and Environment

Master's Thesis 2023  
Department of Space, Earth and Environment  
Division of Energy Technology  
Energy Systems  
Chalmers University of Technology  
SE-412 96 Gothenburg  
Telephone +46 31 772 1000

Cover: Offshore wind farm. Source: Njordr.

Typeset in L<sup>A</sup>T<sub>E</sub>X  
Printed by Chalmers Reproservice  
Gothenburg, Sweden 2023

Wind power with hydrogen production, storage, and reconversion as flexible baseload  
in the Nordic energy system

QUINN SARAH HANITIO

MARÍA ZAS BUSTINGORRI

Department of Space, Earth and Environment

Chalmers University of Technology

## **Abstract**

This thesis aims to investigate the techno-economical feasibility of an offshore wind farm, combined with hydrogen production, storage, and reconversion as a Green Flexible Baseload in southern Sweden in 2030. In the future, it is expected that the share of variable renewable energies (VRE) will increase considerably in Europe, including Sweden and thus, there is a need for balancing technologies in such an energy system with high penetration of VREs. To investigate a concept including hydrogen production, storage, and reconversion in order to balance the inherent variations from wind power, a linear optimization model was developed to find the optimal design of the plant which maximizes the profit by considering the investment and operation of the plant. The work is focused on maximizing the profit made by such a power plant. The hourly operation of the different components is evaluated for a five-year period with real weather data and predicted electricity prices. An inter-year comparison of the designs is then carried out to analyze the effects of wind variations on installed capacity suggestions.

The results show that there are multiple profitable design options for the power plant with different designs of the reconversion technology capacity. One of the main drivers for the overall profitability of the green flexible baseload is the price of hydrogen supplied directly to an assumed industrial demand.

Two final designs are suggested according to the obtained profitability and operational quality results. The proposed designs correspond to the combinations of minimum baseload of 10% in summer to 20% in winter (variable baseload) and minimum baseload of 15% in summer to 15% in winter (constant baseload), both with a grid connection of 72% of the total wind farm capacity.

Keywords: green flexible baseload, wind power, variation management strategies, variability, baseload, techno-economical analysis.



# Acknowledgements

We would like to thank our supervisor, Simon, for all the help throughout this work. For teaching us how to grow within the "three boxes" and develop our academic and professional skills. Thank you to the people at Njordr for offering us the great opportunity of working with them, showing us the creativity and endless opportunities that engineering can offer. Thank you to the department, for being our second home throughout this thesis, for the great fika on Fridays and for the amazing people that it hosts.

---

Thank you Quinn, for always being there, through the good days and the bad ones, always snack and bloopers in hand. From beginning of the master's until the end, I'm really happy you've been there. Al grupito de mis perros culiaos, gracias por las risas, los descansos de café y las birritas post curro. Ha sido un placer conoceros, compartir estos meses con vosotros, y (espero) poder llamaros amigos. Thank you too to all the friends that've been there with me these past two years. Mamá, papá y los peques Zas gracias por darme el privilegio de y ayudarme a perseguir mis sueños en Suecia.

María Zas Bustingorri, Göteborg, June 2023

Thank you María for staying with me in this academic journey called a Master's degree, from the first day (literally) to the last. Always appreciated your presence and ideas. Thank you to my family for entrusting and enabling me to go to another corner of the world to pursue my dreams. Also, thank you to my friends who has been with me throughout this journey and hopefully many more. And above all, to God. By His grace, I am where I am now. Soli Deo gloria.

Quinn Sarah Hanitio, Göteborg, June 2023



# List of Acronyms

Below is the list of acronyms that have been used throughout this thesis listed in alphabetical order:

BL	Base Load
CAPEX	Capital Expenditure
CCGT	Combined Cycle Gas Turbine
GFB	Green Flexible Baseload
LCOE	Levelized Cost of Electricity
LRC	Lined Rock Cavern
OCGT	Open Cycle Gas Turbine
PEM	Proton Exchange Membrane
SDG	Sustainable Development Goals
VRE	Variable Renewable Energy
VMS	Variation Management Strategies
WF	Wind Farm



# Nomenclature

Below is the nomenclature of indices, sets, parameters, and variables that have been used throughout this thesis.

## Indices

$p$	Indices for technological component
$t$	Index for time step

## Sets

$T$	Set of time steps
$P$	Set of components of the system

## Parameters

$WP_t$	Normalized wind production
$price_t^{el}$	Price of electricity
$\eta_p$	Efficiency of components
$IC_p$	Investment cost of components
$VC_{p,t}$	Variable O&M cost of components
$FC_p$	Fixed O&M cost of components
$a_p$	Annuity of components
$CS$	Capacity subsidy
$CR$	Cost reduction

---

$cost^{fuel}$	Price of biofuel
$price^{industry}$	Price of hydrogen sold to industry
$D^{H_2}$	$H_2$ demand
$BL_{min}, BL_{max}$	Base Load minimum and maximum
$r^{inj}, r^{withd}$	Injection and withdrawal rate of H2 storage
$H^{2,cycles}$	Rock cavern cycles

## Variables

$TP$	Total Profit
$c_p$	Capacity of components
$e_t^{industry}$	Hydrogen to industry at each timestep
$e_t^{H_2}$	Hydrogen to gas turbine at each timestep
$e_t^{fuel}$	Fuel to gas turbine at each timestep
$s_t^{charge}, s_t^{discharge}$	Charge and discharge of storage at each timestep

# Contents

<b>List of Acronyms</b>	<b>ix</b>
<b>Nomenclature</b>	<b>xi</b>
<b>List of Figures</b>	<b>xv</b>
<b>List of Tables</b>	<b>xvii</b>
<b>1 Introduction</b>	<b>1</b>
1.1 Variable Renewable Energy . . . . .	1
1.2 Electricity sector in Sweden . . . . .	3
1.3 Project description and objectives . . . . .	6
1.4 Scope . . . . .	6
<b>2 Green Flexible Baseload</b>	<b>7</b>
2.1 Offshore Wind Farm . . . . .	8
2.2 Electrolyzer . . . . .	10
2.3 Hydrogen Storage . . . . .	11
2.4 Hydrogen Reconversion . . . . .	12
<b>3 Method</b>	<b>15</b>
3.1 Model Description . . . . .	16
3.1.1 Sets . . . . .	16
3.1.2 Parameters . . . . .	16
3.1.3 Variables . . . . .	18
3.1.4 Objective Function . . . . .	19
3.1.5 Constraints . . . . .	19
3.2 Assumptions & Input data . . . . .	21
3.2.1 Time-dependent data . . . . .	23
3.2.2 Component's data . . . . .	25
3.3 Scenarios . . . . .	26
3.4 LCOE Analysis . . . . .	27

<b>4</b>	<b>Results</b>	<b>31</b>
4.1	Scenario 1: No minimum baseload . . . . .	31
4.2	Scenario 2: Enforced minimum baseload . . . . .	34
4.2.1	LCOE analysis of Scenario 2 . . . . .	41
4.2.2	Operation of designs . . . . .	42
4.2.3	Robustness analysis of designs . . . . .	48
<b>5</b>	<b>Discussion</b>	<b>53</b>
5.1	Future work . . . . .	55
<b>6</b>	<b>Conclusion</b>	<b>57</b>
	<b>Bibliography</b>	<b>59</b>
<b>A</b>	<b>Details of capacity mix Scenario 1</b>	<b>I</b>
<b>B</b>	<b>Details of capacity mix Scenario 2</b>	<b>III</b>

# List of Figures

1.1	Comparison of electricity production in Germany over a week in 2012 and 2020. With a higher share of renewables (right image) there is no space for baseload. Volker Quaschnig, HTW Berlin . . . . .	2
1.2	Division of the electricity areas in Sweden. Source: Svenska kraftnät . . . . .	3
1.3	Evolution of energy generating technologies in Sweden. Source: Energimyndigheten [13] . . . . .	4
2.1	Green Flexible Baseload schematic representation of plant design and its different components. . . . .	8
2.2	Green Flexible Baseload concept, wind production in grey vs electricity supplied to the grid in green. . . . .	8
2.3	Variations in offshore wind power production, year 2018. Data from Njordr. . . . .	9
2.4	Load duration curve of offshore wind power production for 5 different years in the same location. Data from Njordr. . . . .	10
2.5	Fundamentals of PEM electrolysis. Taken from [25]. . . . .	11
2.6	The schematic diagram for a simple gas turbine. Taken from [41]. . . . .	13
3.1	Schematic representation of GFB model simulated in GAMS, including flexible fuel mixing in the gas turbine. . . . .	15
3.2	Flexibility in H <sub>2</sub> supply to industry, bounded area between upper and lower limit (150% and 45%, respectively). . . . .	22
3.3	Step-function of investment costs associated with the capacity of grid connection as of today. . . . .	23
3.4	Yearly wind power production and electricity price for the year 2018. . . . .	24
3.5	Schematic Power Plant representation with the identification of the main three sections considered. . . . .	28
4.1	Capacity mix of the power plant at different amounts of grid connection ( $BL_{max}$ ) and hydrogen prices . . . . .	32
4.2	Distribution of the power plant profit in scenario 1 (no minimum baseload) for a five-year period. . . . .	33

4.3	Distribution of the power plant profit in scenario 2 with different minimum baseload scenarios for a five-year period. . . . .	35
4.4	Scenarios in which the GFB component of the power plant is profitable	36
4.5	Revenue required in order to make the GFB reach a break-even point, as a percentage of the investment cost of the GT . . . . .	37
4.6	Capacity mix of the power plant at different minimum baseload ( $BL_{min}$ ) scenarios and a hydrogen price of 2.4 €/kg . . . . .	37
4.7	Capacity mix of the power plant at different minimum baseload ( $BL_{min}$ ) scenarios and a hydrogen price of 3 €/kg . . . . .	38
4.8	Capacity mix of the power plant at different minimum baseload ( $BL_{min}$ ) scenarios and a hydrogen price of 4 €/kg . . . . .	38
4.9	Capacity mix of the GFB components with BLmin 10/20% at 5 different year scenarios and a hydrogen price of 4 €/kg. (a. Electrolyzer, CCGT, and OCGT capacities. b. Storage capacity) . . . . .	40
4.10	5-year period load duration curve of the power plant operation with BLmin 10/20%, BLmax = 72% and hydrogen price of 4 €/kg. . . . .	43
4.11	5 year period load duration curve of the power plant operation with BLmin 10/20%, BLmax = 72% and hydrogen price of 4 €/kg. . . . .	44
4.12	Yearly electricity supply of the power plant for 2016 with BLmin 10/20%, BLmax = 72% and hydrogen price of 4 €/kg. . . . .	45
4.13	Electricity supply of the power plant for July 2016 with BLmin 10/20%, BLmax = 72% and hydrogen price of 4 €/kg. . . . .	46
4.14	Electricity supply of the power plant for January 2016 with BLmin 10% to 20%, BLmax = 72% and hydrogen price of 4 €/kg. . . . .	46
4.15	Hydrogen storage level, hydrogen production in the electrolyzer and electricity prices for January 2016 with BLmin 10/20%, BLmax = 72% and hydrogen price of 4 €/kg. . . . .	48
4.16	Hydrogen utilization in the gas turbines and supply to industry for January 2016 with BLmin 10/20%, BLmax = 72% and hydrogen price of 4 €/kg. . . . .	48
4.17	Load duration curve of the power plant operation with BLmin 10/20% with 3 different year scenarios and a hydrogen price of 4 €/kg . . . . .	49
4.18	Load duration curve of the power plant operation with BLmin 15/15% with 3 different year scenarios and a hydrogen price of 4 €/kg . . . . .	50

# List of Tables

2.1	Fuel cell and hydrogen-fueled gas turbine CAPEX and efficiency comparison [36] [35]. . . . .	13
3.1	Efficiency, normalized investment, fixed O&M and variable O&M costs of the multiple components of the power plant. . . . .	25
3.2	Initial input for the proposed power plant. . . . .	26
3.3	Values assigned to the input parameters of the sensitivity analysis. . .	27
4.1	LCOE analysis of Scenario 1 at different hydrogen prices, for $BL_{max} = 100\%$ . . . . .	34
4.2	LCOE analysis of different $BL_{min}$ combinations in Scenario 2 at a hydrogen price of 2.4 €/kg, for $BL_{max} = 72\%$ . . . . .	41
4.3	LCOE analysis of Scenario 2 at a hydrogen price of 3 €/kg, for $BL_{max} = 72\%$ . . . . .	41
4.4	LCOE analysis of Scenario 2 at a hydrogen price of 4 €/kg, for $BL_{max} = 72\%$ . . . . .	42
4.5	Yearly profit breakdown of the power plant with $BL_{min}$ 10% to 20% and $BL_{min}$ 15% to 15% cases. . . . .	51
A.1	Details of the capacity mixes in Scenario 1: no minimum baseload with a maximum grid connection of 42% . . . . .	I
A.2	Details of the capacity mixes in Scenario 1: no minimum baseload with a maximum grid connection of 72% . . . . .	I
A.3	Details of the capacity mixes in Scenario 1: no minimum baseload with a maximum grid connection of 100% . . . . .	I
B.1	Details of the capacity mixes in Scenario 2: Enforced minimum baseload with a hydrogen price of 2,4 €/kg and $BL_{max} = 72\%$ and $BL_{max} = 72\%$ III	III
B.2	Details of the capacity mixes in Scenario 2: Enforced minimum baseload with a hydrogen price of 3 €/kg and $BL_{max} = 72\%$ . . . . .	III
B.3	Details of the capacity mixes in Scenario 2: Enforced minimum baseload with a hydrogen price of 4 €/kg and $BL_{max} = 72\%$ . . . . .	IV



# 1

## Introduction

The Sustainable Development Goals (SDG) have set a path to address the challenges faced by the world with set objectives for 2030. Among many others, Goal 7: access to affordable, reliable, sustainable, and modern energy for all, is expected to play a major role in the near future [1]. The global trend points towards continuous growth and development of the population, which translates into a predicted increase in global electricity demand ranging from 5900 TWh to 7000 TWh by 2030 according to different studied scenarios [2]. On the other hand, in complying with the Paris Agreement, a reduction of CO<sub>2</sub> emissions, the primary driver for global climate change, is necessary in order to maintain global temperature rise below 2°C [3]. Following this development, the European Commission's Green Deal has set a goal of reducing net greenhouse gas emissions by 55% by 2030 [4].

According to the IPCC (2014), the major source of CO<sub>2</sub> emissions is the electricity sector, which contributed around 25% of the overall emissions [5]. Therefore, decarbonizing the electricity sector will play a major role in the fight against climate change. To do so, a transition is necessary from the current energy system based on fossil fuels to a system based on renewable sources, such as wind or solar power, that do not run out or emit polluting gases.

### 1.1 Variable Renewable Energy

Renewable energy has experienced a rise in electricity production share in the past decades [6], and in order to fulfill the mentioned goals, it is expected to further increase (from 28,7% share in 2021 to 60,9% globally in 2030 in a Net Zero Scenario, which aims for no emissions in the year 2050 [7]). Due to the variable nature of renewable technologies, caused by weather dependencies, the expected future electricity production will be irregular. Historically, energy supply is characterized by three types of loads: base load, which is a constant supply of electricity throughout the whole year; mid load, which is supplied intermittently throughout long periods of time; and peak load, which occurs during short periods of time and covers oc-

## 1. Introduction

---

currences of high peaks of demand. With an increasing share of variable renewable energy (VRE) in the system, there will be periods where electricity production exceeds the demand. This scenario takes over and suppresses the role of the baseload, as this constant electricity production will be interrupted due to the VRE supply which has lower operational costs [8]. These effects are already noticeable and are likely to become more frequent in a future electricity system with a higher share of VRE. An example of this scenario can be observed in Figure 1.1, which shows the German electricity system in 2012 (left image) compared with 2020 with higher VRE penetration (right image). In the 2020 scenario, there is no room for a baseload technology, such as nuclear, to produce energy constantly due to the high share of VRE.

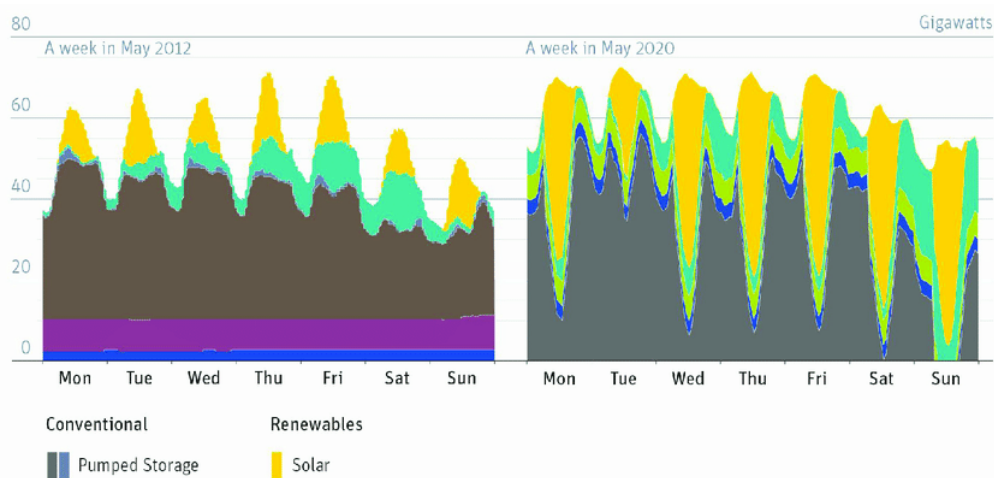


**Figure 1.1:** Comparison of electricity production in Germany over a week in 2012 and 2020. With a higher share of renewables (right image) there is no space for baseload. Volker Quaschnig, HTW Berlin

Baseload generation technologies are characterized by their inflexible operation capabilities along with high costs to change their load, and low operational costs once they are running. An example of such technology is nuclear power plants. The high costs and ramp-up and ramp-down times associated with the turning on and off of these plants make it infeasible to shut them down repeatedly in short timeframes when VRE technologies are generating sufficient electricity to fully cover the demand. Nowadays, in such a situation, the VRE technologies will set the marginal cost of electricity and since their operational costs are very low, other baseload technologies such as nuclear will be running at a loss in these hours. In a future system with larger shares of VRE in electricity production, this loss will be unsustainable. Therefore, multiple solutions are being sought to allow for a reliable and sustainable energy supply, that complies with SDG Goal 7. These solutions, also known as variation management strategies (VMS), exist on both the supply

and demand side. Some of the options available were in the fields of demand-side management (DSM), supply-side management, energy storage, grid infrastructure, electricity market management, sector coupling, and grid ancillary services as discussed by Lund et. al. [9].

## 1.2 Electricity sector in Sweden

Increase in VRE shares is happening globally, including also Sweden, which is the focus in this work. The future Swedish electricity system is divided into four price bidding areas, designated SE1 in the north to SE4 in the south (Figure 1.2), and has connections with neighboring countries in the Nordics and the Baltic Sea region [10]. The areas were divided according to the location of bottlenecks in the transmission capacity. Price differences between bidding areas occur when the transmission capacity between the areas is fully utilized. In southern Sweden (SE3 and SE4), electricity prices tend to be higher than in northern Sweden (SE1 and SE2) since most of the consumption is in the southern part of the country whereas most of the electricity generation is located in the northern part. Thus, the southern price areas are exposed to a greater extent to the electricity prices of mainland Europe via import and export, where the prices are generally higher than average Swedish electricity prices.



**Figure 1.2:** Division of the electricity areas in Sweden. Source: Svenska kraftnät

## 1. Introduction

As per 2022, almost half of Sweden’s electricity production came from hydropower, with the second largest technology being nuclear. Solar and wind power as VREs made up around 20% of the electricity production, with conventional thermal-based power plants fulfilling the rest [11]. In 2040, Sweden has a target of having 100% of its energy production from renewable sources, and nuclear power [12]. The potential for hydropower expansion in Sweden is limited. Due to its nature, hydropower plants can only be built at certain locations with suitable geographical and hydrological features. In addition, the dam and reservoir required for most forms of hydropower production also have an significant impact on the environment, including those of the landscape and local ecosystem, and even potential social impacts. Therefore, in order to meet the 2040 goal, other generation technologies must be developed, and therefore, successful management of VRE and exploring the options to enable the use of VREs as a baseload is crucial.

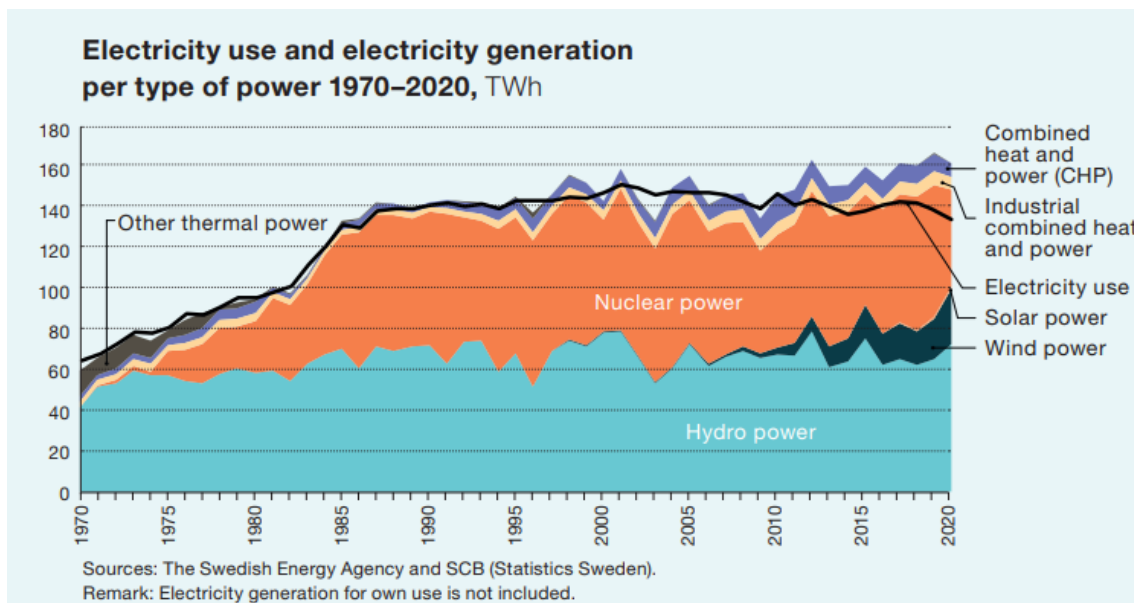


**Figure 1.3:** Evolution of energy generating technologies in Sweden. Source: Energimyndigheten [13]

Wind power as one of the VREs, comprised 19% of the electricity produced in Sweden in 2022 [11] and has increased its share significantly during the past decade (See Figure 1.3). Wind power generation is the renewable energy technology with the highest growth, with a 17% increase in generation capacity in 2021 compared to 2020. Due to the nature of the wind itself, wind power is characterized by high variability and as such, its utilization to provide electricity to consumers is commonly complemented by other energy sources alongside methods to help manage the variability.

There are 2 types of wind power: onshore and offshore. Lately, in Sweden, a country

with large share of wind power, further expansion of onshore wind has been met with some resistance due to its impact on the landscape, and therefore offshore wind is an option being explored for the future. There are several applications for offshore wind farm projects from several companies all around Sweden's coast, amounting to a theoretical potential of 350 TWh per year if all of those applications are realized [14]. This number in reality will likely be lower due to limitations in permits and electricity demand, but it shows the significant potential of Sweden for offshore wind power-generation. In the present day, Swedish Wind Energy Association projected that in 2040, annual offshore wind power production will reach around 45 TWh [15]. With the added load from the current trend in industry electrification, offshore wind can contribute significantly to support future demands of electricity.

There have also been some problems with the electricity grid in recent years which have manifested themselves in the form of electricity price spikes. This was caused by increasing electricity consumption driven by, among others, the electrification of various sectors such as transport and industry [16]. In the future, when more VREs are introduced into the system, there need to be certain safeguards and initiatives to keep and increase the reliability of the electricity system.

In recent years there has been a push to decarbonize industries to reach climate goals. A number of these industries such as steel and cement are switching to direct electrification-based processes and/or hydrogen-based processes, with the goal being to decarbonize the industry through the availability of low-carbon electricity sources and green hydrogen. Eventually, this will result in a significant impact on the electricity system with the increasing number of production facilities that switch to new processes. Due to its low-carbon and low-cost electricity, Sweden has become a region of interest for these industries to be built. This would further increase the demand of electricity in the country, which could grow to twice as much as in the current day by 2050, reaching as much as 300 TWh per year (150 TWh more than in the present) [17]. In addition, a significant part of these new demand is expected to be located in northern Sweden and this would mean a decrease in electricity transmission from the north to the southern regions. Since the electricity generation sector is almost fully decarbonized in Sweden (See Figure 1.3), this increase in demand will imply a need for the expansion of the current system into larger generation capacities, especially in the south. Several studies such as those conducted by Walter et. al. [18] and Toktarova et. al. [19] show that these demands can be satisfied through VRE such as wind and solar power. Furthermore, supplementations in energy storage systems to VRE have been shown to improve the cost-efficiency of the processes and help manage the inherent intermittency of the VRE. The aim for the future is to solve the reliability problem, perhaps through a combination of variation management strategies, namely demand-side management

(DSM), supply-side management, and energy storage [20].

### 1.3 Project description and objectives

To offer a possible solution to meet the needs of the Swedish electricity system in the future including the possibilities of managing VRE variability, a concept for an offshore wind-based Green Flexible Baseload (GFB) proposed by Njordr Offshore Wind is evaluated. The main goal of this project is to analyze the techno-economic feasibility of the proposed GFB concept, with the aim of helping to manage the variations in a VRE-penetrated energy system. In addition, the GFB will be able to supply green hydrogen to industries. During this project answers will be sought to the following questions:

- What are the factors that affect the economic feasibility of a GFB power plant concept?
- How should the GFB power plant be designed in terms of component sizing with an objective to maximize the power plant revenue?
- How would the chosen power plant designs operate?

### 1.4 Scope

This project is carried out at the Division of Energy Technology, Department of Space, Earth, and Environment at Chalmers University of Technology using site specific data and a proposed plant concept provided by Njordr Offshore Wind AB. The data provided spans around 18 years from 2002 to 2020, and the proposed concept includes Njordr's preliminary estimations of the plant's component sizes and costs.

This thesis consists of a techno-economic analysis of the proposed concept of an offshore wind farm coupled with hydrogen production, storage, and reconversion as a green flexible baseload power plant and does not include real-world commissioning and operation of the plant. Optimization of the sizes for the power plant components is carried out using a linear optimization model in GAMS.

# 2

## Green Flexible Baseload

The concept suggested by Njordr is a supply-side management and energy storage VMS strategy that can contribute to manage variations in a future electricity system with high wind penetration. The idea behind this project is to develop a power plant consisting of a wind farm, an electrolyzer, hydrogen storage, and a reversion technology such as a H<sub>2</sub>-fueled gas turbine. Figure 2.1 represents a schematic view of the suggested plant and its different components.

The purpose of the concept is to mitigate variations of wind power within the power plant. This is done by producing hydrogen during high-wind periods when the electricity price is low and reconvert the hydrogen to electricity during low-wind periods with high electricity prices. Besides the advantages that this idea could bring to the system, such as reducing the variations from wind power electricity, this idea brings an additional benefit through a diversified revenue stream. By supplying electricity with the GFB during high electricity price periods, the power plant will make revenue when otherwise wind would not be available to sell electricity. Additionally, the connection to the grid could be reduced, which means an increased utilization rate of the remaining grid connection, and reduced investment costs. Lastly, the revenue stream from selling hydrogen to the industry can also result in significant profit for the power plant.

This concept is named green flexible baseload since the goal is to continuously supply electricity to the grid (baseload) from renewable energy technologies (green) with flexibility in its operation to produce either hydrogen or electricity (flexible). The suggested idea is displayed in Figure 2.2, where it can be seen that the variable nature of wind power (grey line) is managed into a more constant electricity supply (green line).

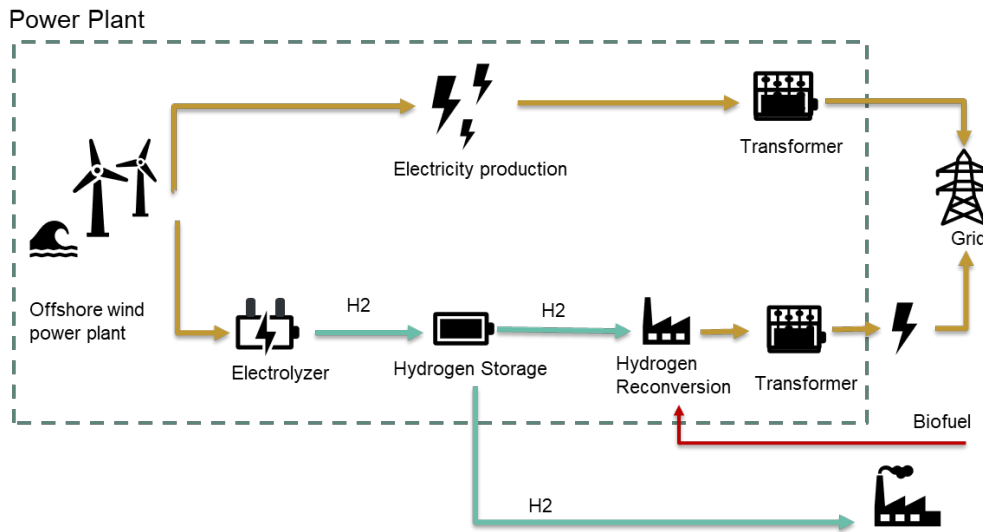


**Figure 2.1:** Green Flexible Baseload schematic representation of plant design and its different components.

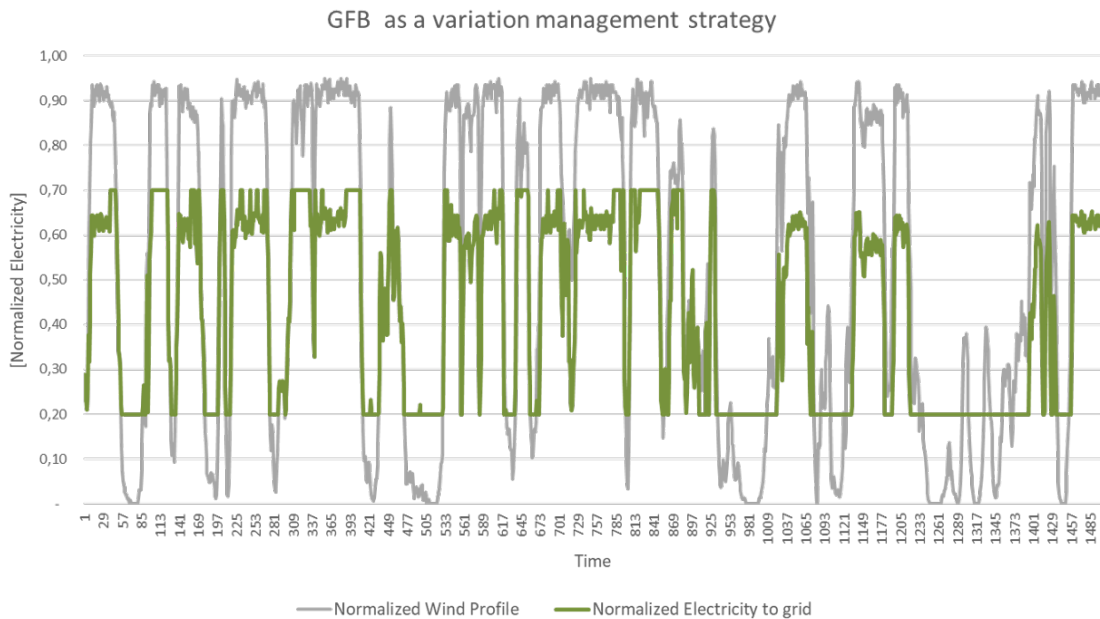


**Figure 2.2:** Green Flexible Baseload concept, wind production in grey vs electricity supplied to the grid in green.

## 2.1 Offshore Wind Farm

This thesis is focused on managing the variations of an offshore wind farm. Offshore wind has some advantages compared to onshore wind. Offshore wind farms are located off the coast, where wind speeds tend to be higher and more continuous

as there are no obstructions at sea. This allows for higher electricity generation potential. It also poses less visual impact on the landscape and does not compete with other purposes in terms of land use, unlike onshore wind. For this reason, offshore wind turbines can be built taller and with a larger rotor, allowing them to sweep through a larger area and capture more wind even at lower speeds. [21]. This combination of higher and more consistent wind speeds with a larger rotor thus result in a higher production capacity, also known as the capacity factor. In the long run, offshore wind has more potential for development as there are no restrictions regarding its size and it does not share the social and environmental complications normally associated with onshore wind farms. On the other side, naturally, given its location, the construction and maintenance of offshore wind farm infrastructure is more complicated than onshore wind and dictates a higher cost [22]. Nevertheless, costs are expected to go down over time as the technology matures and more countries incorporate offshore wind as part of their efforts in increasing renewable power generation.

As with any other VRE, offshore wind has variations in its electricity generation. These variations are characterized by high periods of production, and low ones, taking place on a multi-day or weekly basis. As seen in Figure 2.3, the electricity generation varies drastically on an hourly basis throughout the whole year.

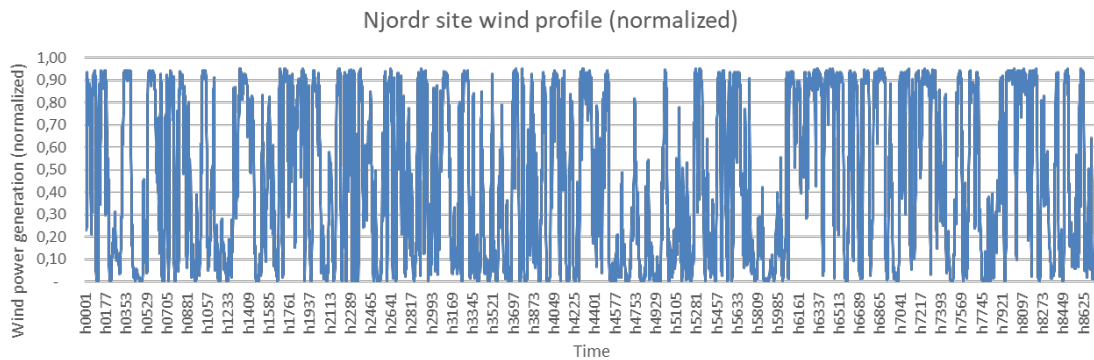


**Figure 2.3:** Variations in offshore wind power production, year 2018. Data from Njordr.

Another characteristic of wind power variations is the significant differences that occur between years. Figure 2.4 displays the load duration curves of wind power production for five different years, all at the same site. As shown in the figure, the inter-annual variations in wind power generation are quite significant. Clearly, the years 2015 and 2019 have a higher amount of full load hours than the year 2010, which is the year with the lowest full load hours. These characteristics dictate that the integration of wind power into the electricity system requires VMS, which is the purpose of the concept being developed.

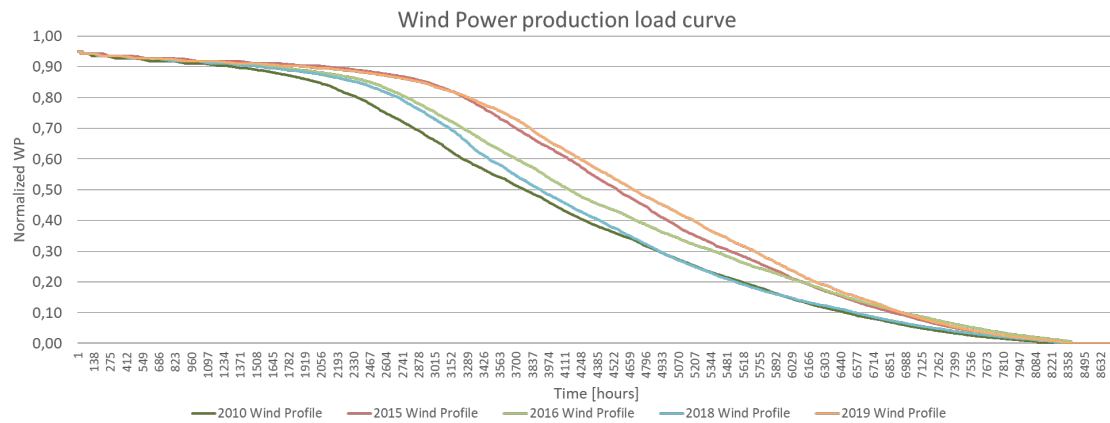


**Figure 2.4:** Load duration curve of offshore wind power production for 5 different years in the same location. Data from Njodr.

## 2.2 Electrolyzer

Hydrogen can be produced by splitting water into oxygen and hydrogen with electricity in a process called electrolysis, a reaction that takes place in an electrolyzer. This technology can be scaled up or down according to its intended use, and different types have been developed and are already available. Electrolyzers are composed of an anode and a cathode separated by an electrolyte. The different types of electrolyte material and the ionic species it conducts determine the types of electrolyzers and their operation [23]. For the GFB two main types of electrolyzers were studied and compared to evaluate their suitability for the power plant.

Alkaline electrolyzers are the more mature technology. Within them, a reaction takes place between two electrodes, separated by a porous membrane, in a liquid electrolyte. On the other hand, proton exchange membrane (PEM) electrolyzers use a solid polymer electrolyte membrane and an electric current to separate hydrogen and oxygen from water [24]. The fundamentals of how PEM electrolyzers function is shown in Figure 2.6.

When selecting the most appropriate technology for the proposed power plant, the relevant characteristics, as well as their predicted development must be considered. Alkaline electrolyzers are currently cheaper and more developed. On the other hand, PEM electrolyzers are better in dynamic power generation [26], smaller in size, and can reach fast dynamic response, but they are more expensive [27]. When considering wind power-generated electricity, PEM electrolyzers become the most suitable technology since they have high efficiencies, short start-up times, and an extensive range of production range variations [28]. These qualities are suitable for the variable nature of wind power generation, allowing for an intermittent production

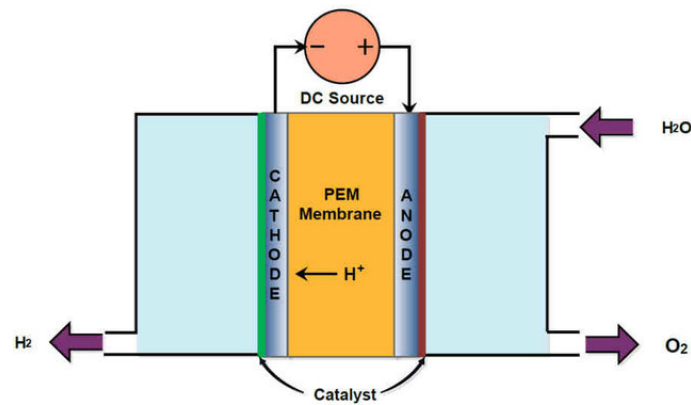


**Figure 2.5:** Fundamentals of PEM electrolysis. Taken from [25].

of hydrogen, when the price and wind conditions are appropriate.

## 2.3 Hydrogen Storage

The produced hydrogen from the electrolyzer can be stored to be withdrawn when required. There are multiple types of storage technologies that can be used: tanks, lined rock caverns (LRC), and salt caverns.

Storing compressed hydrogen in tanks is the most commonly used method of storage [29]. Hydrogen is stored in cylindrical vessels made of a lightweight and low-cost material that can hold the high pressure required for the hydrogen; additionally, it must be able to withstand the diffusion of the compressed gas and the possible embrittlement caused [29].

Although tank storage is the most widespread storage technology, when considering the future predicted scale of hydrogen production, underground storage is considered the most economical and safe option [30],[31]. Underground storage is naturally, due to its overlying geological layers, better protected from external influences such as fire, military or terrorist attacks [30]. Within the underground hydrogen storage of hydrogen, salt caverns and LRC are highlighted.

Salt caverns are underground cavities within salt domes or salt layers done artificially, and they provide great gas tightness and inertness [30]. The gas is purified and compressed before being injected to the caverns [32]. One of the best advantages of these caverns are the unique physicochemical properties of rock salt: lack of water, low porosity and permeability (great sealing capacity), and chemical inertia towards hydrogen, which prevents the contamination of the stored hydrogen [30], [31]. Furthermore, salt caverns occur in thick layers which have great conditions for heat conduction [30]. Moreover, another advantage of salt caverns are their flexible

operation with high injection rates and withdrawal cycles [31]. On the down side, the availability of such storage depends greatly on its geographical availability, as salt caverns are not present all throughout the world.

Another underground, large-scale hydrogen storage are lined rock caverns (LRC), which share some similarities with salt caverns. LRC storage systems are composed of two main facilities, the above-ground facility where the hydrogen is compressed and the operation of the technology controlled, and the underground storage caverns, connected via tunnels.[33]

Rock caverns require a main element in order to contain the hydrogen, the lining. Three main components constitute the lining in LRC storage: a sealing layer that holds the gas within, a pressure-distributing section that distributes the load from the pressurized gas to the rock, and the mass of rock where the caverns are dug, which absorbs the load from the gas pressure [33]. The interaction between these structural components is crucial for the correct functioning of the storage facility, and to prevent leakage.

For the purpose of this project, a lined rock cavern (LRC) hydrogen storage was chosen, as research and current practice show that this technology is the aptest for Swedish conditions. This is due to the lack of salt cavern availability in the Swedish territory [31] and the high costs associated with large-scale hydrogen storage in tanks.

## 2.4 Hydrogen Reconversion

The last component of the GFB concept suggested in this project is the reconversion of hydrogen back to electricity to be supplied to the grid. There are two technologies that can be used for this purpose: fuel cells and hydrogen-fueled gas turbines. For the development of this thesis, hydrogen-fueled gas turbines were selected over the use of fuel cells. This was done due to the higher costs associated with the use of fuel cells, as well as their lower electrical efficiency (See Table 2.1 for comparison). Additionally, fuel cells that run on mixed fuel are unconventional and thermodynamically unstable [34], while hydrogen-fueled gas turbines can run on mixed fuels, enabling the option of a complementary fuel source other than hydrogen [35].

Gas turbines are a common technology used for power generation in the current energy system, and they are most often run on natural gas. For the purpose of the proposed GFB power plant, it is necessary to have a hydrogen-fueled gas turbine. Currently, most gas turbines can operate with at least 30% vol. hydrogen as their fuel without any necessary changes. Higher volumes of hydrogen to fuel the gas turbine result require changes in the burner and combustion chamber design [37].

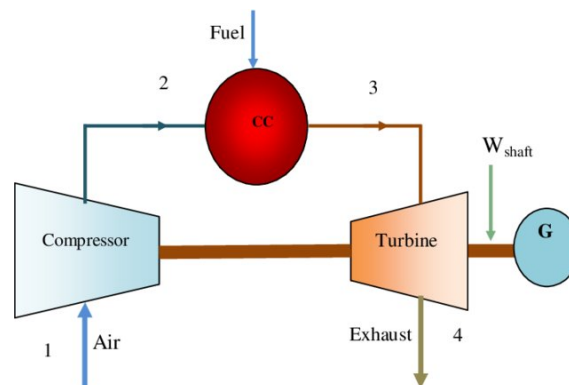
**Table 2.1:** Fuel cell and hydrogen-fueled gas turbine CAPEX and efficiency comparison [36] [35].

Technology	CAPEX [M€/GW]	$\eta$ [%]
Fuel Cell	1100	50
Combined-cycle gas turbine (CCGT)	954	61
Open-cycle gas turbine (OCGT)	805	40

Currently, 100% hydrogen-fueled gas turbines are still being developed by several manufacturers [38]. Considering the time scope of this project, it is assumed that this technology will be already available in the future, and the costs are assumed to be higher than those predicted for regular gas turbines.

Gas turbines have three main components: the compressor, the combustion system, and the turbine. The compressor gathers the input air into the engine and then after pressurizing it, it feeds it into the combustion chamber. There, the fuel is mixed in, where it is burned at high temperatures, creating a stream of hot gas at high pressures, which is then expanded in the turbine. The latter is composed by a series of blades that rotate with the incoming gas flux, making a generator shaft rotate and thus generating electricity [39].

There are two types of gas turbines, open-cycle gas turbines (OCGT), or combined-cycle gas turbines (CCGT). OCGT operates by intaking air and combusting it to then run the turbine, as mentioned above. CCGT starts with an OCGT, then the excess heat from the gas turbine is used to generate steam that expands through a steam turbine, generating additional electricity [40]. This added complexity translates into higher efficiency but also higher costs for the CCGT. The choice between OCGT and CCGT is left to be decided throughout the simulation and modeling of the power plant.

**Figure 2.6:** The schematic diagram for a simple gas turbine. Taken from [41].



# 3

## Method

In this thesis, a techno-economical analysis was done of the proposed GFB power plant presented in the former chapters. This was carried out in two steps: a model optimization, where the sizing of the different GFB components was determined, and an LCOE evaluation of the multiple proposed designs. The mathematical linear optimization model of the power plant was implemented in GAMS, an optimization tool that allows finding the most optimal configurations of the power plant under different scenarios. This chapter provides a mathematical description of the model, Section 3.1, as well as the assumptions made, Section 3.2, and the different studied scenarios, Section 3.3. The economical comparison of the modeled results was done using the levelized cost of electricity as described in Section 3.4.

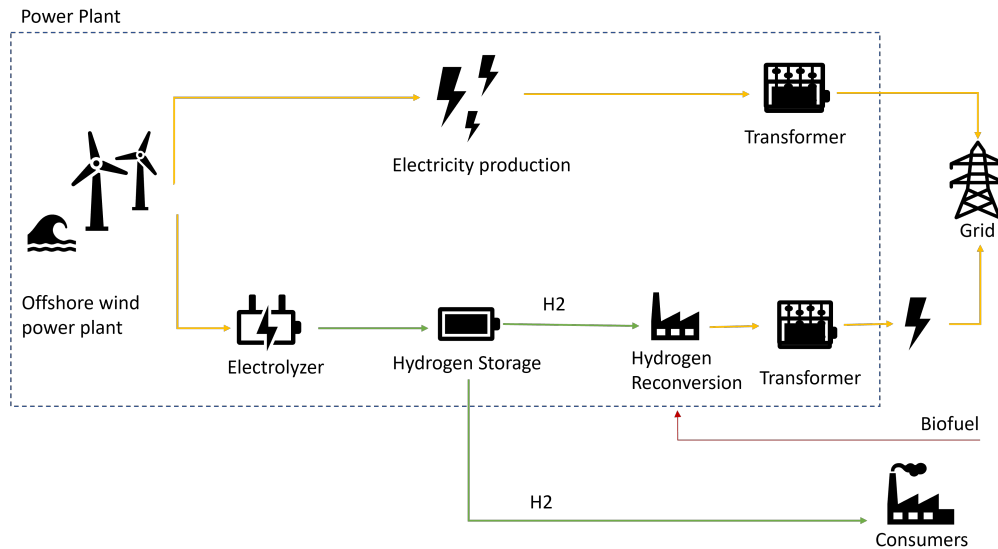


**Figure 3.1:** Schematic representation of GFB model simulated in GAMS, including flexible fuel mixing in the gas turbine.

## 3.1 Model Description

This section displays the mathematical representation of the GFB concept described in the previous chapter. The main goal of this optimization is to determine the design of the different components of the GFB, i.e. the capacities of the electrolyzer, the hydrogen storage and the gas turbine. The most economically feasible design is to be developed, as well as the most optimal operation of the components in order to maximize the total profit made by the power plant.

### 3.1.1 Sets

Sets in linear programming models are considered as the group of data that are of similar type. The sets considered in this linear program are the following:

- Time: all hours in five years -  $\mathbf{T}$
- Components of the system: wind farm (WF), electrolyzer (ELY), hydrogen storage (storage), and gas turbine (GT) both OCGT and CCGT. -  $\mathbf{P}$

The time set ( $\mathbf{t}$ ) for this project was defined as a combination of five different years of weather data. This was done since the inter annual variations are considerable (see Figure 2.4), and thus by combining the years the investments will be made such that more weather events can be handled by the installed capacities. The chosen years were: 2010, 2015, 2016, 2018, and 2019. This set was divided into two subsets, summer time and winter time. Summer time was determined to be the period corresponding to the months of April to September for every year, whereas winter was defined corresponding to the period between October and March of each year. Therefore, for each year within the five year period:  $t_{summer} = 2161 - 6552$  and  $t_{winter} = 0001 - 2160, 6553 - 8760$ .

### 3.1.2 Parameters

Parameters are fixed values used in the optimization program, they are defined in this section. The dependency on each of the sets described previously is noted with the corresponding subscript,  $\mathbf{t}$  or  $\mathbf{p}$ .

The year dependent data used in this project was the following:

- Normalized wind production at any hour (for a five year period) [GWh/G-Winstalled hour] -  $\mathbf{WP}_t$
- Price of electricity at any time  $t$  [€/MWh]-  $\mathbf{price}_t^{el}$

The technical parameters for each component considered in the model are the fol-

lowing:

- Efficiency for every system components p [%]-  $\eta_p$
- Investment cost for every system components p [M€/GW]-  $IC_p$
- Fixed O&M cost for every system components p [M€/GW]-  $FC_p$
- Variable O&M cost for every system components p at any time t [M€/GWh]-  $VC_{p,t}$

Since the analysis carried out is done yearly, the costs must be annualized for each of the components. Therefore, the annuity is another parameter used in this linear model.

- Annuity of each component p -  $a_p$

The annuity is calculated according to Equation 3.1, where  $i$  stands for the interest rate (7%), and  $year_p$  is the lifetime of each component.

$$a_p = \frac{i}{1 - (1 + i)^{-year_p}} \quad (3.1)$$

A reduction in yearly costs is considered for reduced transmission line connections. This concept will be further explained in future sections of this report. This parameter was included in the model:

- Wind farm investment cost reduction for reduced grid connection, per five year period [M€] -  $CR$

Next, the corresponding prices at which the different fuels are sold were determined also as parameters:

- Cost of biomethane used in the gas turbine [€/GWh]-  $cost^{fuel}$
- Price at which H2 is sold to the industry [€/GWh]-  $price^{industry}$

Additionally, a yearly demand of hydrogen from the industry was considered as an additional parameter:

- Demand for H2 in the industry [GWh/year]-  $D^{H2}$

The GFB is characterized by its ability to supply electricity to the grid within certain boundaries. These upper and lower limits were defined as Base Load (BL) minimum and maximum, and they represent a percentage of the installed wind capacity.

- Minimum electricity supply to the grid [%]-  $BL_{min}$

- Maximum electricity supply to the grid [%] -  $BL_{max}$

Lastly, the injection and withdrawal rate of hydrogen into the rock cavern was also defined as a parameter in the linear model. These parameters represent the limitations of the hydrogen storage to charge and discharge hydrogen. Additionally, the maximum yearly cycles for hydrogen storage were included in the model:

- Rate of injection and withdrawal to the rock cavern [fraction of installed capacity]-  $r^{inj}, r^{withd}$
- Maximum yearly cycles for rock caverns [cycles] -  $H_{2,cycles}$

#### 3.1.3 Variables

The variables of a linear optimization are those values which are meant to be optimized in order to reach a certain goal. In the present case, the main objective of this simulation is to maximize the total profit of the power plant during a five year period. Therefore, the total profit is the free variable that is to be optimized.

- Total profit for a five year period [M€]-  $TP$

The rest of the variables used in this model are then calculated by the model, where the most optimal combination of them (according to profit maximization) will be chosen:

- Generation of each component p at any time t (storage generation means storage level) [GWh/hour]-  $g_{p,t}$
- Capacity of each component p [GW]-  $c_p$
- Hydrogen sold to the industry at time t [GWh/hour]-  $e_t^{industry}$
- Energy from H2 used in the gas turbine at time t [GWh/hour]-  $e_t^{H2}$
- Energy from biofuel used in the gas turbine at time t [GWh/hour] -  $e_t^{fuel}$
- Hourly charge and discharge of the hydrogen storage [GWh/hour] -  $s_t^{charge}, s_t^{discharge}$

The electricity being supplied to the grid in this model is defined as the electricity generated by the wind farm that goes directly to the grid, i.e. accounting for the electricity being supplied to the electrolyzer ( $g_{WF,t} - g_{ELY,t}$ ); and the electricity generated by the gas turbine ( $g_{GT,t}$ ).

### 3.1.4 Objective Function

The objective function is the main equation in an optimization model. In this model, the main goal is to maximize the total profit ( $TP$ ) during five years (represented as  $y$ ) considering all the relevant costs and income. The costs of this model include: the investment costs of each component of the plant ( $IC_p$ ), their fixed and variable O&M costs ( $FC_p$  and  $VC_p$ ), which account for the five year period ( $y = 5$ ), and the cost of injecting biofuel into the gas turbine ( $e_t^{fuel} \cdot cost^{fuel}$ ). The revenue made by the plant is comprised of the electricity sold to the grid ( $(g_{WF,t} + g_{GT,t} - g_{ELY,t}) \cdot price_t^{el}$ ), the income made from selling hydrogen to the industry ( $e_t^{industry} \cdot price^{industry}$ ), and the cost reductions from reduced transmission connections ( $CR$ ).

$$\begin{aligned}
 TP = & \sum_{t \in T} (g_{WF,t} + g_{GT,t} - g_{ELY,t}) \cdot price_t^{el} + \sum_{t \in T} e_t^{industry} \cdot price^{industry} \\
 & - \sum_{p \in P} IC_p \cdot a_p \cdot c_p \cdot y - \sum_{p \in P} FC_p \cdot c_p \cdot y - \sum_{p \in P} \sum_{t \in T} VC_p \cdot g_{p,t} - \sum_{t \in T} e_t^{fuel} \cdot cost^{fuel} + CR \cdot a_{grid} \cdot y
 \end{aligned} \tag{3.2}$$

### 3.1.5 Constraints

The following equations determine the constraints of the optimization model and take into account the different characteristics of each component as well as the time limitations.

Considering the definition of GFB, upper and lower limits on the supplied electricity to the grid are set ( $BL_{min}$  and  $BL_{max}$ ). The electricity supplied to the grid is that generated from the gas turbine ( $g_{GT,t}$ ), along with the electricity produced by the wind farm ( $g_{WF,t}$ ), without the portion of the wind farm-produced electricity that is being used for the electrolyzer ( $g_{ELY,t}$ ). This supplied electricity is bounded as follows:

$$BL_{min} \leq g_{WF,t} + g_{GT,t} - g_{ELY,t} \leq BL_{max} \quad \forall t \in T \tag{3.3}$$

The total wind production at any time  $t$  ( $g_{WF,t}$ ) should be smaller than or equal to the wind farm capacity ( $c_{WF}$ ) times the available wind at that time  $t$  ( $WP_t$ ):

$$g_{WF,t} \leq WP_t \cdot c_{WF} \quad \forall t \in T \tag{3.4}$$

The generation of the components ( $g_{p,t}$ ) cannot exceed their capacity ( $c_p$ ), this is a redundant constraint for the wind farm:

$$g_{p,t} \leq c_p \quad \forall t \in T, p \in P \quad (3.5)$$

A balancing equation is required to determine the storage status, where the storage at any time  $t$  ( $g_{storage,t+1}$ ) is equal to the available storage before ( $g_{storage,t}$ ) plus the net charge of the electrolyzer, defined by:  $s_t^{charge} - s_t^{discharge}$

$$g_{storage,t+1} = g_{storage,t} + s_t^{charge} - s_t^{discharge} \quad \forall t \in T \quad (3.6)$$

A storage usage constraint must be determined to limit the rate at which the hydrogen is injected ( $r^{inj}$ ) and withdrawn ( $r^{withd}$ ) from the caverns.

$$\frac{s_t^{charge}}{r^{inj}} + \frac{s_t^{discharge}}{r^{withd}} \leq c_{storage} \quad \forall t \in T \quad (3.7)$$

Another limitation characteristic of hydrogen storage is the number of cycles ( $H_{2,cycles}$ ) of charges that can be experienced per year:

$$\sum_{t \in T} \eta_{storage} \cdot s_t^{charge} \leq c_{storage} \cdot H_{2,cycles} \cdot y \quad \forall t \in T \quad (3.8)$$

Where  $\eta_{storage}$  is the storage efficiency,  $c_{storage}$  its capacity, and  $s_t^{storage}$  is charging rate. The factor 5 is used to account for the five year period being considered.

The charge ( $s_t^{charge}$ ) and discharge ( $s_t^{discharge}$ ) rates of the hydrogen storage can never exceed its capacity ( $c_{storage}$ ):

$$s_t^{charge}, s_t^{discharge} \leq c_{storage} \quad \forall t \in T \quad (3.9)$$

Another constraint of the system is defined by the amount of hydrogen being sold to the industry ( $e_t^{industry}$ ), which each year throughout the five year period cannot exceed the total yearly hydrogen demand of the industry ( $D^{H2}$ ).

$$\sum_{t \in year} e_t^{industry} \leq D^{H2} \quad \forall t \in T \quad (3.10)$$

Similarly, the hydrogen sold to the industry at any time  $t$  ( $e_t^{industry}$ ) has an upper and lower limitation according to the yearly demand ( $D^{H2}$ ). This constraint is established to represent a flexible demand from the industry side, the upper and lower limits being named  $H_{2,max}$  and  $H_{2,min}$ , respectively.

$$\frac{D^{H2}}{8760} \cdot H_{2,min} \leq e_t^{industry} \leq \frac{D^{H2}}{8760} \cdot H_{2,max} \quad \forall t \in T \quad (3.11)$$

In addition, the model must ensure that the hydrogen produced in the electrolyzer ( $g_{ELY,t} \cdot \eta_{ELY}$ ) is greater than the net charge of the storage ( $s_t^{charge} - s_t^{discharge}$ ) and the hydrogen being used at any time  $t$  either for the gas turbine ( $e_t^{H2}$ ) or sold to the industry ( $e_t^{industry}$ ).

$$g_{ELY,t} \cdot \eta_{ELY} \geq s_t^{charge} - s_t^{discharge} + e_t^{industry} + e_t^{H2} \quad \forall t \in T \quad (3.12)$$

The amount of fuel required by the gas turbine ( $g_{GT,t}/\eta_{GT}$ ) is defined by the energy being supplied in the form of hydrogen from the storage ( $e_t^{H2}$ ) plus the energy from the bio fuel being injected into the gas turbine ( $e_t^{fuel}$ ):

$$\frac{g_{GT,t}}{\eta_{GT}} \leq e_t^{H2} + e_t^{fuel} \quad \forall t \in T \quad (3.13)$$

A limitation on the amount of biomethane ( $e_t^{fuel}$ ) used in the gas turbine was set to be 10% of the total fuel requirement during the five year period ( $g_{GT,t}/\eta_{GT}$ ):

$$\sum_{t \in T} e_t^{fuel} \leq 0.1 \cdot \sum_{t \in T} g_{GT,t} \quad \forall t \in T \quad (3.14)$$

## 3.2 Assumptions & Input data

This section presents the relevant assumptions made throughout the development of the model. Additionally, relevant input data used during the simulations is also introduced.

Since the main goal of the optimization model is to maximize profit, the revenue streams of the power plant play a major role. One of the main revenues from the GFB components is the supply of hydrogen to industry. Determining the price at which hydrogen will be sold in the future is uncertain, as most studies focus on the production costs. Additionally, it is likely that the price will vary throughout the year and even hourly. Therefore, to simplify the scenarios, it was assumed that the price of hydrogen ( $price^{industry}$ ) remains constant throughout the year. Considering that the projected retail price of hydrogen to industry in a near future ranges from 5-7€/kg in 2030 [42], the chosen values were selected to be below these predictions to account for the possibility of prices being on the lower end of the estimations. The scenarios were evaluated considered three hydrogen prices: 2.4, 3, and 4€/kg.

### 3. Method

It was assumed that there would be an existing demand of hydrogen from the industry, therefore this creates an additional revenue stream for the GFB. This demand was set to 60 000 tons of hydrogen yearly, and the supply was assumed to be flexible. Assuming high flexibility is possible for the supply of hydrogen to industry, the maximum and minimum hydrogen supply limits to industry were set to be  $H_{2,max} = 150\%$  and  $H_{2,min} = 45\%$  of the constant annual demand [43]. A simple representation of these limits is shown in Figure 3.2, where the upper and lower boundaries are shown.

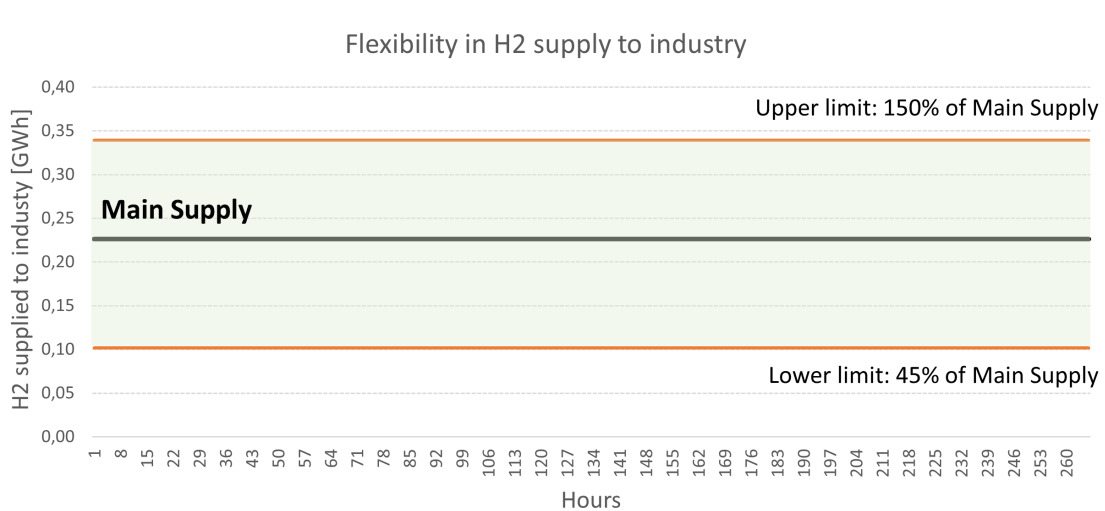


**Figure 3.2:** Flexibility in H2 supply to industry, bounded area between upper and lower limit (150% and 45%, respectively).

As stated in the model description, the main goal is to maximize the total profit from the power plant. Therefore, considering the revenue streams is crucial for the analysis. The wind farm investment costs (See Table 3.1) include the costs for connecting to the electricity grid. The largest transformer for grid connection is 1.4 GW [44], and it corresponds to an investment cost of 300 M€. Since the wind farm investment costs include the connection costs, assuming 100% grid connection is installed, there exists a potential value on a reduced grid connection for the power plant. Figure 3.3 displays these associated cost reductions, where blocks of 1.4 GW are subtracted from the grid connection capacity, with the benefit of a lower capital cost for the wind farm. For the presented model, these costs are discounted from the reference wind farm investment costs as the cost reductions  $CR$  in the objective function. During the modeling, the connection to the grid is translated into the upper limit for the base load ( $BL_{max}$ ).

Considering the stepwise cost of connection to the grid, the values for  $BL_{max}$  were determined accordingly.  $BL_{max}$  is a percentage of the installed wind farm capacity

and the maximum supply of electricity to the grid (i.e., the connection capacity to grid). Assuming that if an investment into a connection step is made, the maximum capacity of that step will be used, then the possible values for the upper electricity supply limit become:  $BL_{max} = 44\%, 72\%, 100\%$ .

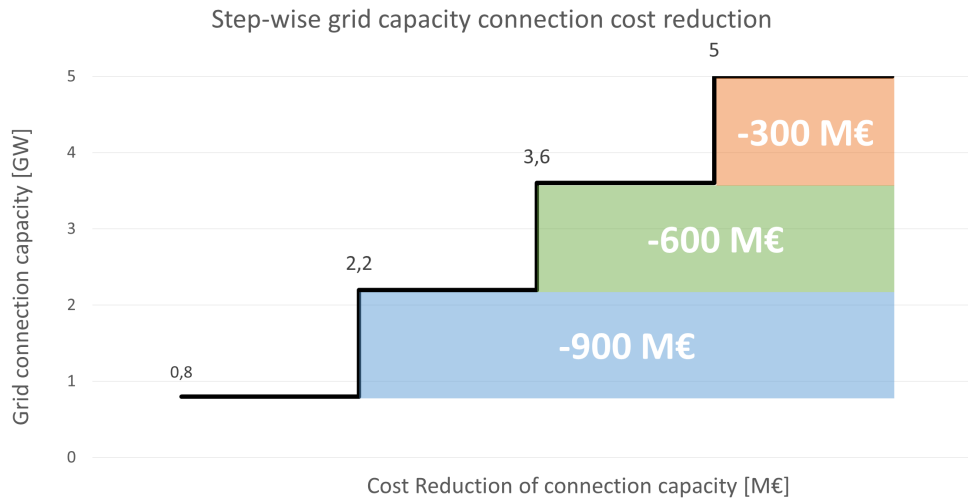


**Figure 3.3:** Step-function of investment costs associated with the capacity of grid connection as of today.

Lastly, another important cost to be taken into account is the one associated to the additional fuel used in the gas turbines to reconvert hydrogen to electricity. For the purpose of this thesis, it was considered that the additional fuel used for combustion is biomethane, at a constant cost of  $cost^{fuel} = 0,06 \text{ M€}/\text{GWh}$  [35].

### 3.2.1 Time-dependent data

When presenting the assumptions, it must be clarified that the model was developed for a five year period as a mean to include the impact of inter-annual variations in the results. As discussed in previous chapters, wind variations are too significant from year to year to generalize with a single one. When evaluating a single year the individual component capacities are designed in perfect accordance with the occurrences of the year. Therefore the results are too precise and specific to the particular year being identified. To avoid possible significant design differences between years, the multi-year time set was chosen.

The yearly data is part of the most relevant input of the present model. During the simulation, an hourly wind profile,  $WP_t$ , was used to determine the hourly wind farm electricity production during five years. The available wind profile was provided by Njordr for a specific off-shore location in Southern Sweden. This data was available for 20 years, between 2000 and 2020.

### 3. Method

The electricity prices,  $price_t^{el}$ , used in this model are taken from predictions simulated for the year 2040. These predictions were obtained with Simon Öberg's model, which uses specific weather data to derive an approximation of the future marginal cost profile for electricity in the near future (2040) with the assumed evolution of the electricity system. The data used represents the costs per unit of electricity generated, but in this model, these costs were assumed to be the electricity prices at which the generated electricity is to be sold. Predicted costs from 2040 were used since, considering the time frame and expected project development, the studied GFB plant should be in operation around that time frame.

As the electricity prices used are predictions of future costs and therefore quite theoretical, real-life market limitations are not considered. Currently, there is a maximum price cap on electricity, which prevents prices from exceeding too large values, and therefore electricity generators can at any hour charge as maximum that set price. This cap has changed throughout the years and is set according to the current market and electricity situation. Considering historical data and estimations on future electricity caps [45], [46], the electricity prices were limited to a maximum of 300€/MWh at any time.

Since large amounts of data were available, the considered data was reduced to a five year period. The data for years 2010, 2015, 2016, 2018, and 2019 was chosen for most of the analysis carried out. These years data was used for both the wind profile and the predicted electricity prices (which depend on the specific year weather data). The yearly distribution of the wind power production ( $g_{WF,t}$ ) and electricity prices for 2018 are displayed in Figure 3.4. It can be observed that there are periods of low wind power generation and high electricity prices, providing a convenient scenario for the GFB to operate.

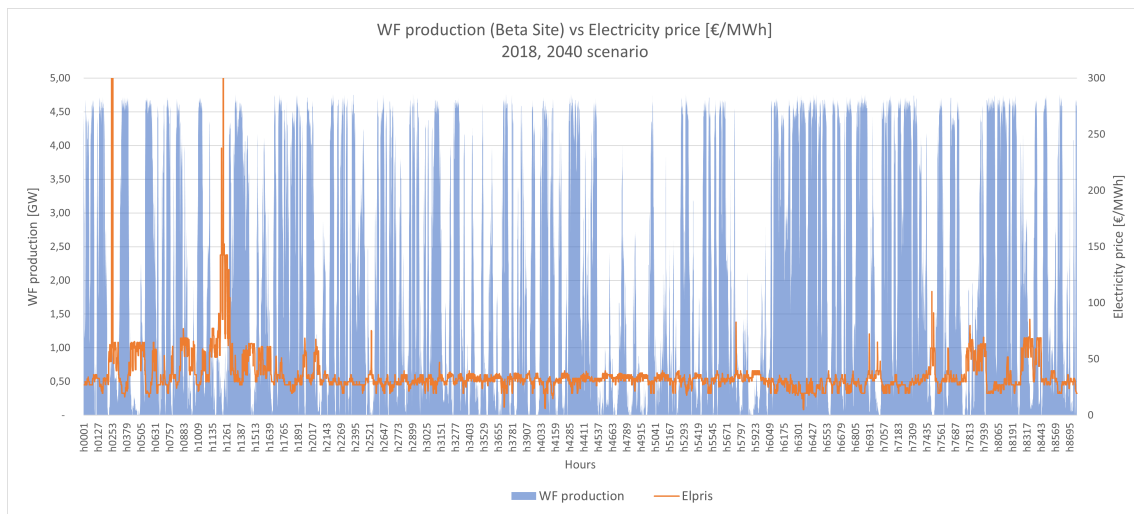


**Figure 3.4:** Yearly wind power production and electricity price for the year 2018.

### 3.2.2 Component's data

As previously stated, one of the main components of the power plant is the wind farm, and all other aspects of the plant being designed accordingly. Therefore, in line with the estimations made by Njordr, the wind farm capacity in this project was fixed to  $c_{WF} = 5GW$ .

The technical data used for each component is displayed in Table 3.1. Considering that the costs will go down as the technology evolves in the future, the predicted costs for the year 2040 were used in this project. Technical data for the wind farm, electrolyzer, hydrogen storage, open-cycle gas turbine, and combined-cycle gas turbine were obtained from the Danish Energy Agency Technology Catalogues ([36], [47],[48]). In addition, to better adjust to the project estimates, the efficiency of the open-cycle gas turbine was taken from the initial project estimates from Njordr [49] and corroborated by the data used by Öberg [37]. The efficiency of the hydrogen storage is also calculated to account for the energy requirement from the compression (not included in the model).

To adjust for the difference between the current gas turbine fuel mix capability and the ones considered in this project, the cost data for the gas turbines was increased by 115%, considering that the gas turbines are assumed to have 100% hydrogen mixing ratio capability. This means that the fuel input can be anywhere between 0% hydrogen mix or 100%. The estimated additional costs for the turbines were obtained from Öberg's work [35], which assumes that the cost of such turbines will be 115% of the current costs.

**Table 3.1:** Efficiency, normalized investment, fixed O&M and variable O&M costs of the multiple components of the power plant.

Component	$\eta_p$ [%]	$IC_p$ [M€/GW]	$VC_p$ [M€/GWh]	$FC_p$ [M€/GW]	Lifetime [years]
Wind Farm	0,95	1645	39	0,004	30
Electrolyzer	0,65	650	45,5	0	25
H2 Storage	0.88	2	0	0	100
OCGT	0,40	805	18,6	0,002	25
CCGT	0,61	954	27,8	0,004	25

As stated in Section 3.1, some assumptions about the hydrogen storage were done. First, the hydrogen storage cycles,  $H_{s,storage}$ , were set to 20, according to the work done by Öberg [35]. Additionally, the injection and withdrawal rates were assumed to be  $r^{inj} = \frac{1}{40}$  and  $r^{withd} = \frac{1}{20}$  of the installed hydrogen storage capacity respectively.

### 3.3 Scenarios

As mentioned before, the model carried out was developed to maximize the overall profit. Since the GFB section is seen as an addition to the planned 5GW wind farm, when analyzing the profitability, only the profit of the GFB and the associated costs of its components are considered. Since there was no full knowledge about the electricity market behaviour and the effect of this power plant on the system, it was decided to disregard the direct costs of the wind farm (investment costs, variable and fixed Operation and Maintenance costs) in the model part of the method, allowing for a more in-depth analysis of the GFB concept.

When performing the analysis of the model, different scenarios were taken into account. Initially, the suggested input (See Table 3.2) was used in the model. As will be seen in the following chapter, this particular design is not economically feasible. Therefore, different scenarios and a sensitivity analysis were created to better study the proposed power plant.

**Table 3.2:** Initial input for the proposed power plant.

Parameter	Input data
Wind Farm	5 GW
BLmin	20%
BLmax	72%
H2 price	2,4€/kg
H2 demand	60 000 tons

The chosen parameters for the sensitivity analysis of the model included the upper and lower limits of electricity supply ( $BL_{min}$ ,  $BL_{max}$ ) and the hydrogen price which the industry will pay for the hydrogen inflow ( $price^{industry}$ ). Since these values are main design drivers for the model, and the hydrogen price will play a major role in the profitability of the concept, and is a rather unpredictable value for the future years. Taking this into consideration, the different scenarios were chosen for further evaluation.

#### Scenario 1: No baseload minimum

As a first analysis of the model presented, the model was given complete freedom to invest in different capacities of the aforementioned technologies which together constitute the GFB power plant. In this first analysis, the minimum supply of electricity to grid was suppressed, i.e.  $BL_{min} = 0\%$ . The evaluation of the model was focused on the profitability and design characteristics of this model, when there

is no minimum supply imposed.

The design differences are directly related to the other parameters. Therefore,  $BL_{max}$  was chosen to be 44, 72, and 100% of the installed wind farm capacity, while the price of hydrogen to industry was altered between 2,4, 3, and 4 €/kg.

### Scenario 2: Baseload minimum requirement

The next analysis performed was a sensitivity analysis that included all the parameters mentioned in this section. In contrast with the previous case, this evaluation included a requirement for a minimum supply of electricity to the grid ( $BL_{min}$ ). Additionally, some flexibility in this minimum was assumed; allowing for a lower supply during the summer months ( $BL_{min,summer} \leq BL_{min,winter}$ ). This was done since the overall demand for electricity during the summer is lower than that during winter, wind profiles are also lower during the summer, and maintaining a constant baseload minimum is more expensive to fulfill. The different values implemented during the sensitivity analysis are displayed in Table 3.3.

**Table 3.3:** Values assigned to the input parameters of the sensitivity analysis.

Parameter	Values for sensitivity analysis
$BL_{min,summer}$ - $BL_{min,winter}$	10-10, 10-15, 10-20, 15-15, 15-20, 20-20 %
$BL_{max}$	44, 72, 100 %
$price^{industry}$	2.4, 3, 4 €/kg

The combination of these different values results in a total of 54 possible sub-scenarios for Scenario 2 ( $6 \times 3 \times 3$ ). Since the different  $BL_{min,summer}$ - $BL_{min,winter}$  combinations are evaluated for every  $BL_{max}$  and every  $price^{industry}$ .

Similar as in the previous scenario, the main objective of this analysis is to evaluate the design and its profitability. Additionally, for the non-profitable scenario, an analysis on the required subsidy for installed capacity ( $CS$ ) in a capacity market was performed. In other words, the necessary subsidies were determined to make the non-profitable models economically feasible.

## 3.4 LCOE Analysis

The Levelized Cost of Electricity (LCOE) is used as a measurement of the average net present cost of electricity generation for a particular generation technology. It is normally used to compare different generation technologies. It represents the average cost of a unit of electricity generated. The LCOE of a 5 GW offshore wind power plant is used as a comparison with the newly computed LCOE for the overall

### 3. Method

concept, including WF and GFB, and split into the wind farm and GFB sections. Since the model developed has a five-year resolution, and thus results are for this period of time, the LCOE calculated throughout this thesis is done for five years instead of during the lifetime of the power plant. Therefore the simplified version of the LCOE formula used is:

$$LCOE = \frac{\text{Total Costs}}{\text{Total electricity supplied}} \quad (3.15)$$

When calculating the LCOE of the proposed power plant, the different elements of the plant had to be taken into account. Therefore three main sections of the power plant were identified, as illustrated in Figure 3.5: the whole plant (red box), the WF (blue box), and the additional GFB section (green box). In the figure, the generated electricity from the WF supplied to the grid is denoted  $WF_{el}$ , while the electricity generated from the GFB to the grid is named  $GFB_{el}$ . On the bottom part,  $REV_{H_2}$  refers to the total revenue made from  $H_2$ , and  $COST_{biofuel}$  indicates the total cost from purchasing the additional biofuel to run the GT.

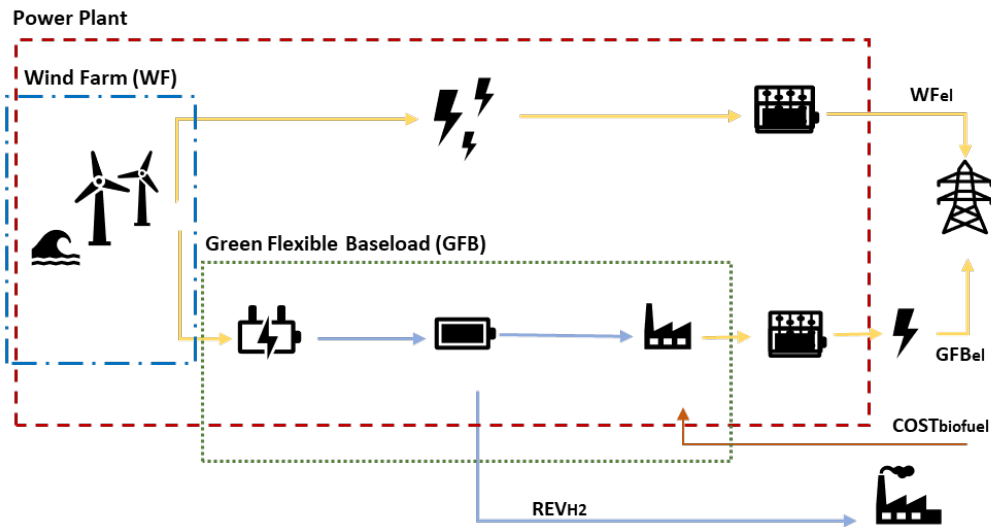


**Figure 3.5:** Schematic Power Plant representation with the identification of the main three sections considered.

Another aspect to consider during this analysis is the incoming revenue from hydrogen being sold to the industry. Two approaches were proposed for how to manage this revenue flow in the analysis: firstly, subtracting the profit made from selling hydrogen from the costs, thus the LCOE is the average price to cover the remaining costs. On the other hand, LCOE was also calculated by considering hydrogen as a byproduct of the system and therefore not accounting for it during the calculations.

The former approach is indicated with a  $H_2$  subscript:  $LCOE_{H_2}$ ; whereas the latter is indicated with a 0 as subscript:  $LCOE_0$ .

When computing the LCOE of the whole power plant, considering hydrogen as a revenue stream ( $LCOE_{plant,H_2}$ ), Equation 3.16 was used. The cost reductions associated to the grid connection capacity were deducted from the total costs ( $CR \cdot a_{WF}$ ).

$$LCOE_{plant,H_2} = \frac{\sum \text{Total cost of components} - REV_{H_2} + COST_{biofuel} - CR \cdot a_{WF} \cdot y}{WF_{el} + GFB_{el}} \quad (3.16)$$

Similarly, if the LCOE of the whole power plant is computed when hydrogen is considered as a byproduct ( $LCOE_{plant,0}$ ), the formula used becomes:

$$LCOE_{plant,0} = \frac{\sum \text{Total cost of components} + COST_{biofuel} - CR \cdot a_{WF} \cdot y}{WF_{el} + GFB_{el}} \quad (3.17)$$

When analyzing the WF section on its own, only the costs of the WF and the electricity supplied directly from it to the grid ( $WF_{el}$ ) are considered, as well as the cost reductions due to limitations in grid connection. Since the revenue from selling hydrogen does not affect this section of the power plant, it is not accounted for.

$$LCOE_{WF} = \frac{\sum \text{Total cost of WF} - CR \cdot a_{WF} \cdot y}{WF_{el}} \quad (3.18)$$

Lastly, when computing the LCOE of the GFB, the costs of the WF, the electricity directly supplied from the WF to the grid, and the cost reductions associated with the capacity of connection to the grid are not accounted for. When considering hydrogen revenue in the analysis,  $LCOE_{GFB,H_2}$ , the used formula is:

$$LCOE_{GFB,H_2} = \frac{\sum \text{Total cost of GFB} - REV_{H_2} + COST_{biofuel}}{GFB_{el}} \quad (3.19)$$

While, if hydrogen is considered as a byproduct the used formula becomes Equation 3.20.

$$LCOE_{GFB,0} = \frac{\sum \text{Total cost of GFB} + COST_{biofuel}}{GFB_{el}} \quad (3.20)$$



# 4

## Results

This chapter presents the results obtained throughout the analysis of this model in two scenarios: with no minimum baseload requirement set and with an enforced minimum baseload.

When evaluating the results of the model, the main objective was to determine the most techno-economically feasible design of the GFB to maximize the overall profit, as this is an additional extension that is assumed to be added to an already-planned wind farm (thus the fixed wind farm capacity). Therefore, the main focus was set on determining the profitability, design characteristics, and operation of only the GFB section of the power plant (See Figure 3.5).

### 4.1 Scenario 1: No minimum baseload

An analysis was carried out for the first scenario, where no baseload minimum was imposed on the system. The description of the different parameters used during the analysis is presented in Section 3.3, namely the different values for the grid connection ( $BL_{max}$ ) and the hydrogen prices ( $price^{industry}$ ). Taking into account that the hydrogen price might be fluctuating in the future, and that this has been selected according to predictions, the initial focus was set on the most economically optimal grid connection for the system.

The model was given the freedom to invest in the most profitable capacities of each of the components of the GFB (refer to Appendix A for further detail), but as seen in Figure 4.1, the model decides not to invest in the reconversion technology whatsoever, regardless of the hydrogen price. This takes place for all prices of hydrogen being sold to industry, which translates into the supply of hydrogen having a higher economic value for the power plant than the supply of electricity when wind production is insufficient and electricity prices are high. In this case, the wind farm is behaving as a hydrogen producer rather than a GFB supply.

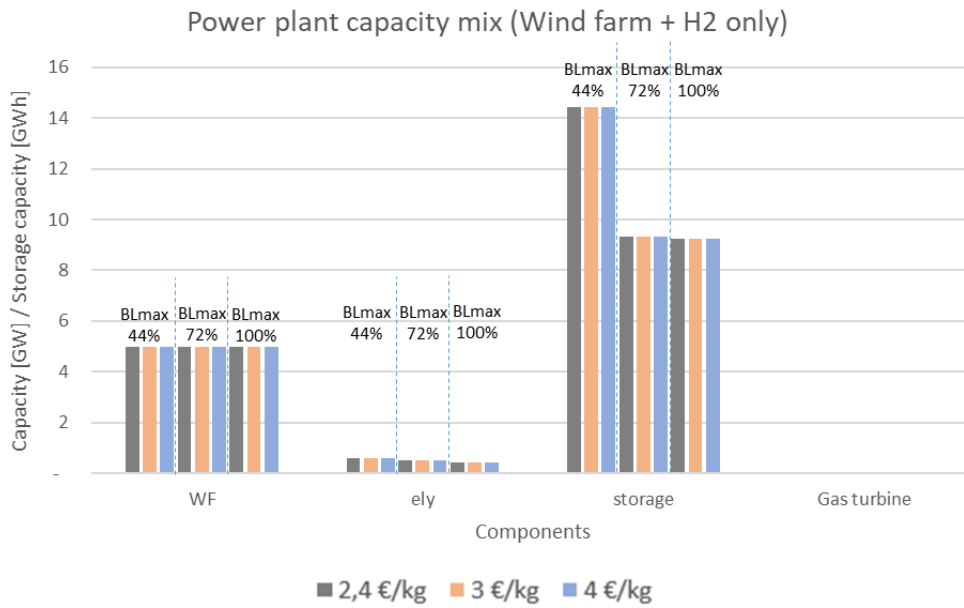


**Figure 4.1:** Capacity mix of the power plant at different amounts of grid connection ( $BL_{max}$ ) and hydrogen prices

Figure 4.1 shows the capacity mixes of the power plant for different grid connection capacities ( $BL_{max}$ ) and hydrogen prices. It can be seen that the capacity mix is not affected by the variations in hydrogen prices and is only affected by the amount of grid connection ( $BL_{max}$ ). In the case of 44%  $BL_{max}$ , the storage size required is higher than in scenarios with higher  $BL_{max}$ , since the limited capability to supply electricity to the grid means that the model wants to sell as much electricity as possible every hour (since reconverting the electricity in the GT is not profitable enough). Therefore, hydrogen production in the electrolyzer is stopped in periods of high electricity prices so the plant can make the most profit, since the supply to industry must be met, larger storage is needed if the electrolyzer is going to operate less hours. The capacity mix also only slightly differs between the 72% and 100%  $BL_{max}$ .

The profitability of the power plant for all the studied scenarios is displayed in Figure 4.2. As observed from the trend of the results in Figure 4.2, the most economically feasible cases for this scenario, regardless of the price of hydrogen, correspond to a grid connection of  $BL_{max} = 100\%$ , although it is notable that the profit made is higher by a small margin compared to the case with  $BL_{max} = 72\%$ . This is likely caused by the fact that even though the high electricity prices are not sufficiently large to justify the investment into a reconversion technology (Figure 4.1), they are large enough to compete against the cost reductions from connectivity. This means that there are sufficient high electricity price hours in which there is enough

electricity being generated by the wind farm to use the remaining 28% connection to the grid.

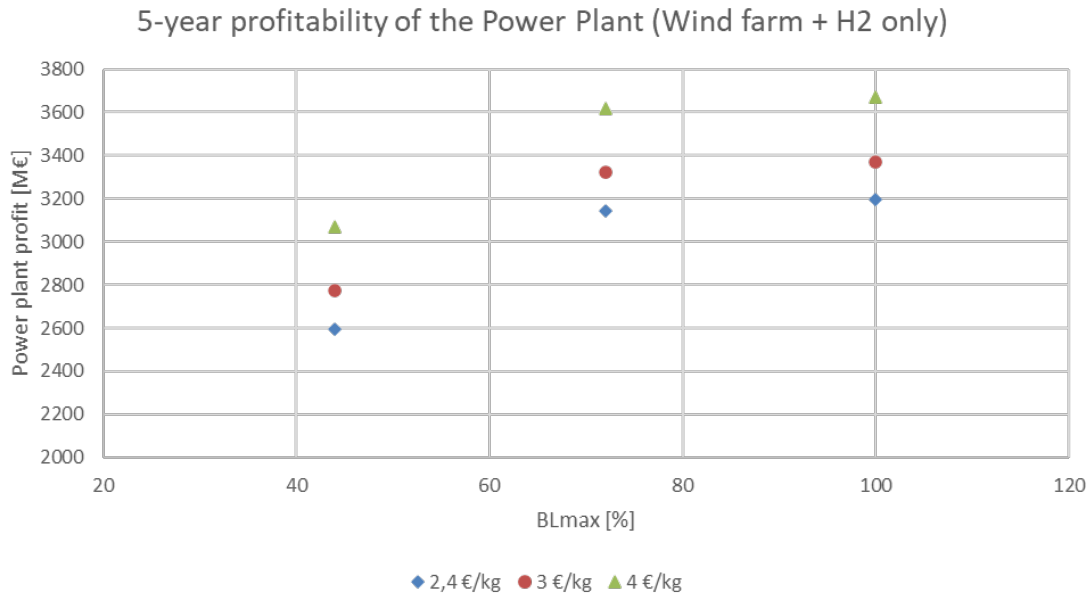


**Figure 4.2:** Distribution of the power plant profit in scenario 1 (no minimum baseload) for a five-year period.

Lastly, an analysis of the LCOE was performed for this scenario. As a basis for comparison, LCOE for a 5 GW offshore wind farm was first calculated using the wind profile of the site provided by Njordr. This is done to establish a baseline and assess how the LCOE changes with every addition made to the power plant. When calculating the LCOE of the standalone wind farm (meaning that there is no hydrogen demand from industry) and assuming all produced electricity is being sold to the grid, it was found that the LCOE for the data used in this project is:  $LCOE_{ref} = 44.6\text{€}/MWh$ . This calculation was done according to Equation 3.18.

For Scenario 1, there is no GFB electricity generation, therefore only  $LCOE_{WF}$ ,  $LCOE_{PP,H2}$ , and  $LCOE_{PP,0}$  were calculated in this scenario. Since it was determined that the most economically feasible connection to the grid for this scenario is  $BL_{max} = 100\%$ , all results for  $BL_{max} = 44\%$  and  $BL_{max} = 72\%$  were disregarded for this analysis.

Table 4.1 displays the obtained results for the LCOE analysis of Scenario 1. The first observation that can be made from these results is that the  $LCOE_{WF}$  is higher compared to the  $LCOE_{ref}$  when there is only a 5 GW wind farm. This is due to the imposed demand from industry, which forces the model to supply less electricity directly from the wind farm to the grid and instead supply it to the electrolyzer, thus resulting in a smaller denominator in Equation 3.18 and results in overall higher

$LCOE_{WF}$  than the original LCOE. When evaluating the power plant as a whole, the need to supply hydrogen to industry forces the model to invest in electrolyzer and storage; expensive components that increase the total costs of the power plant and thus the  $LCOE_{PP,0}$ . The last column,  $LCOE_{PP,H2}$ , includes the revenue of the hydrogen sold to the industry, which has a significant impact on the LCOE. As expected and observed in the table below, the higher the revenue of hydrogen, corresponding to a higher price, results in a lower LCOE. It is interesting to note from the last column, that the obtained  $LCOE_{PP,H2}$  is smaller than the wind-only case. This takes place since the revenue made from selling hydrogen is so much larger than the costs of the GFB that said profit compensates for some of the wind farm costs, thus the numerator of Equation 3.16 becomes smaller than for the wind-only case. The cost per unit of electricity generated is smaller than the wind-only case since the profit made from selling hydrogen is so significant.

**Table 4.1:** LCOE analysis of Scenario 1 at different hydrogen prices, for  $BL_{max} = 100\%$ .

Hydrogen Price	$LCOE_{WF}$ [€/MWh]	$LCOE_{PP,0}$ [€/MWh]	$LCOE_{PP,H2}$ [€/MWh]
2.4 €/kg	51.37	53.89	46.01
3 €/kg	51.36	53.88	44.03
4 €/kg]	51.36	53.88	40.75

## 4.2 Scenario 2: Enforced minimum baseload

Scenario 2 was the enforced minimum baseload scenario, where different combinations of  $BL_{min,summer}$  and  $BL_{min,winter}$  were imposed on the model to ensure a minimum supply of electricity to the grid at every hour of the year, hence fulfilling the function of a baseload. Figure 4.3 displays the profit made by the power plant in the different studied cases. For this particular scenario, it can be seen that the most profitable cases are those with a grid connection of 72%. This is because by imposing a minimum supply to the grid at every hour, the power plant is forced to diverge some of the produced electricity from the wind farm to the electrolyzer to generate enough hydrogen for both the industry and the reconversion technology. Therefore, having a higher capacity of connection but not having enough electricity from the wind farm (since it is being used in the electrolyzer) implies investing in a grid connection capacity that is not going to be used, thus  $BL_{max} = 100\%$  is less profitable. On the other hand, having a grid connection corresponding to  $BL_{max} = 44\%$ , although it reduces the CAPEX of the wind farm by 600M€, is not economically beneficial for the power plant. This connection is too small for the size

of the wind farm being installed, and the costs of the GFB section are too large to justify a deviation of the electricity from being supplied to the grid directly from the wind farm into the electrolyzer.

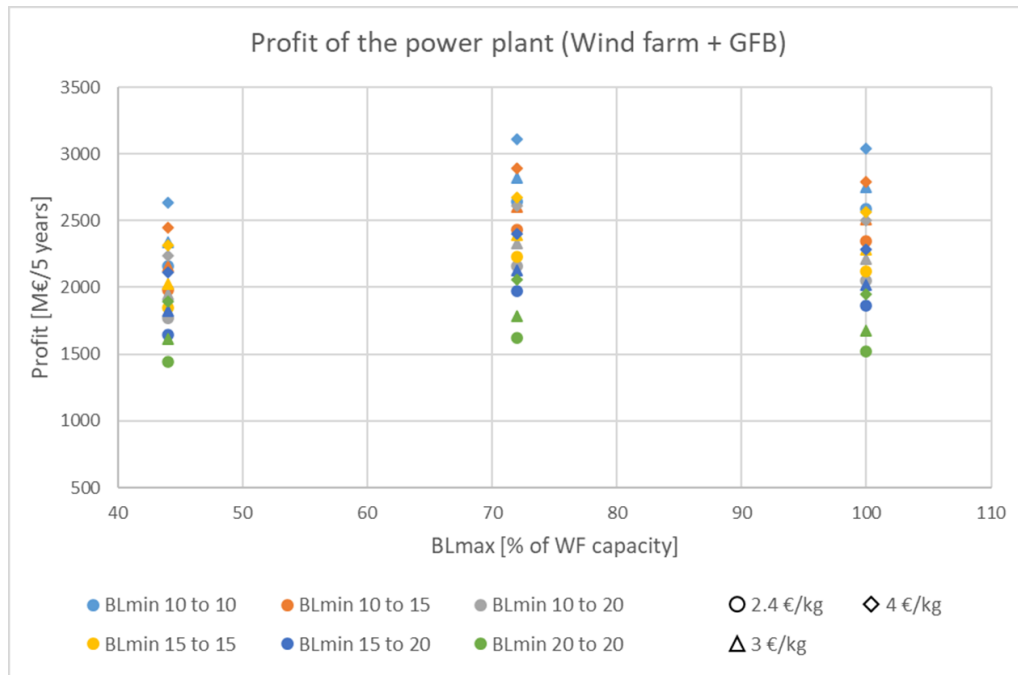


**Figure 4.3:** Distribution of the power plant profit in scenario 2 with different minimum baseload scenarios for a five-year period.

It is important to note that in this analysis only the profitability of the GFB component is evaluated without taking into account the costs and revenue of the wind farm. This is done in order to evaluate the economic feasibility of the GFB concept on its own. Economic comparison with the wind farm included will be further discussed in the LCOE analysis in Section 4.2.1.

In this scenario, it is interesting to see the variability of profitability between each particular case according to the different studied parameters. Since it was determined that for this scenario, a  $BL_{max} = 72\%$  is most economically beneficial, the following results will only represent those particular cases. Figure 4.4 displays the profitability of the GFB section of the power plant for each case at different studied hydrogen prices.

## 4. Results

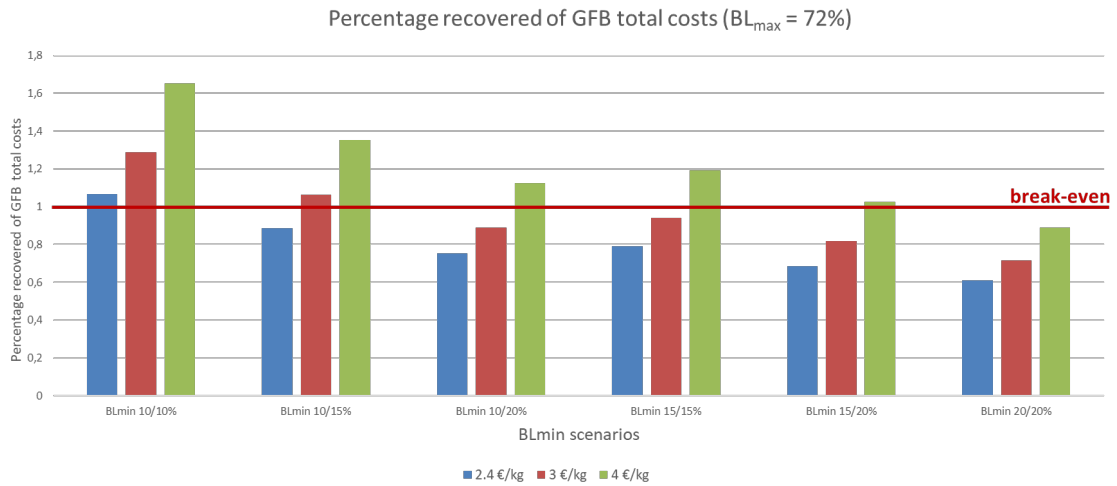


**Figure 4.4:** Scenarios in which the GFB component of the power plant is profitable

From Figure 4.4, it can be observed that there are some profitable scenarios based on the minimum baseload and hydrogen prices. The profitability is displayed as a percentage that shows the ratio between the obtained revenue of the GFB section (i.e., the electricity sold from the gas turbine and the sold hydrogen to industry), and the total costs of the GFB section (its different components and the costs of purchased fuel). The break-even line is indicated in red, where the GFB obtained enough revenue to fully recover all its costs. When considering these results, is important to emphasize that since all calculations include an interest rate of 7%, the profitability calculations include a risk factor which translates into actual higher revenue; therefore even at the break-even point, profit is being made.

As seen in Figure 4.4 there are some designs that are profitable on their own, while others do not break even. The lack of revenue from the latter is highlighted in Figure 4.5, where the needed amount to break even is shown as a percentage of the total investment costs of the GT. In a future scenario, this gap to break-even could be covered by some sort of subsidy, or be partially covered by a capacity market in which electricity suppliers are compensated for the available capacity installed to generate electricity when the system requires it. The needed revenue varies depending on the  $BL_{min}$  combinations and hydrogen prices, ranging from 23,6% to 172,2% of the gas turbines' CAPEX in the evaluated cases. Furthermore, the profit needed for break-even is calculated on a five-year basis, which implies that in higher  $BL_{min}$  cases (when the subsidy represents a large percentage of the CAPEX of the reconversion technology), the profit required is not sustainable in the long term, as most likely no government or investor would be willing to pay such large amounts to cover the gap to break-even.

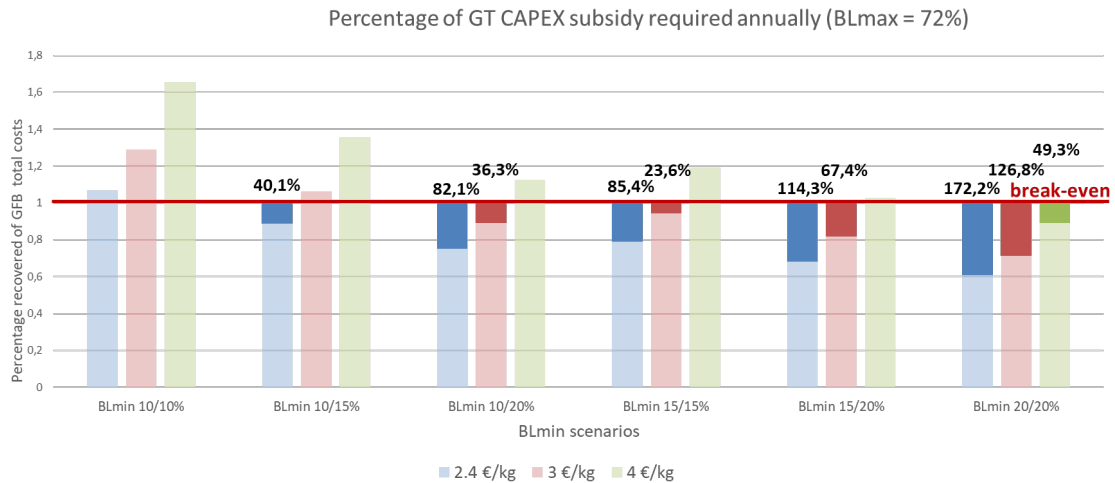


**Figure 4.5:** Revenue required in order to make the GFB reach a break-even point, as a percentage of the investment cost of the GT

Figures 4.3, 4.4, and 4.5 also show that lower  $BL_{min}$  combinations are preferable economically. To further investigate the reason for the different amounts of profitability and hence the capacity subsidies, a breakdown of the installed capacity mix determined by the model was mapped. Figures 4.6, 4.7, and 4.8 displays the different installed capacities for each of the studied cases of Scenario 2 at hydrogen prices of 2.4, 3, and 4 €/kg and a constant  $BL_{max} = 72\%$ .

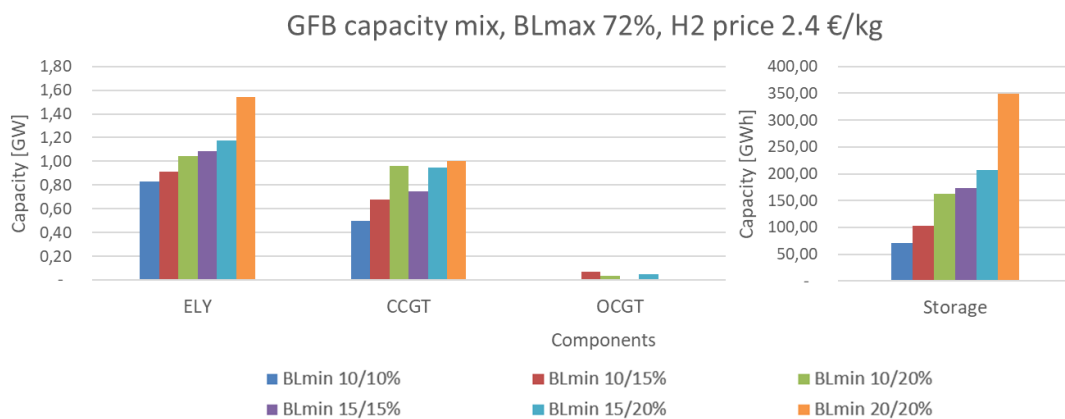


**Figure 4.6:** Capacity mix of the power plant at different minimum baseload ( $BL_{min}$ ) scenarios and a hydrogen price of 2.4 €/kg

## 4. Results

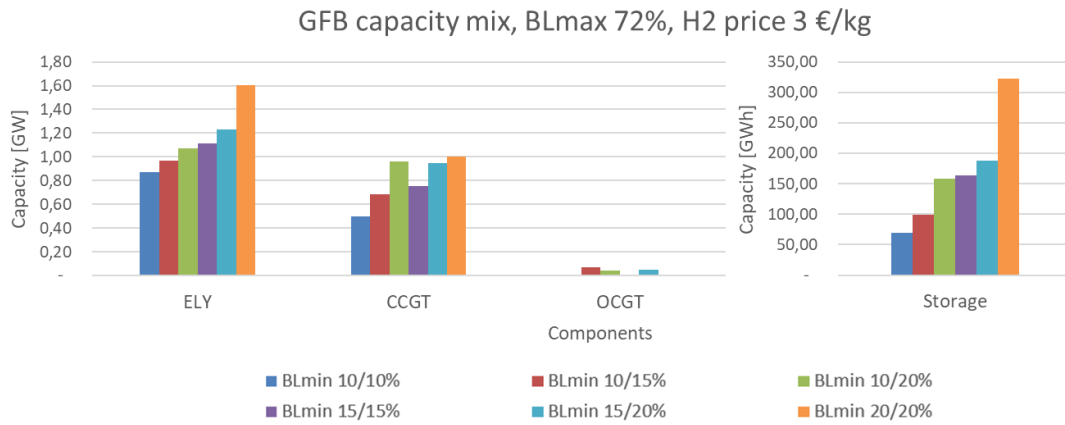


**Figure 4.7:** Capacity mix of the power plant at different minimum baseload ( $BL_{min}$ ) scenarios and a hydrogen price of 3 €/kg

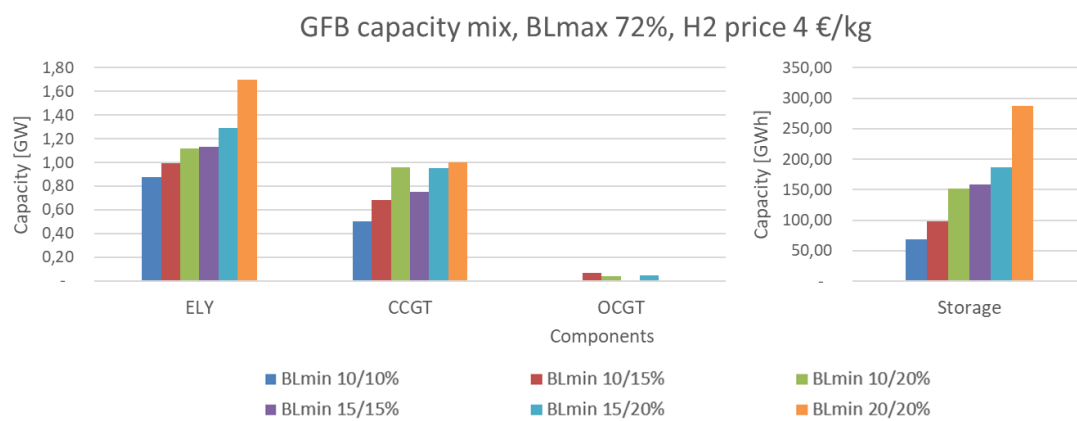


**Figure 4.8:** Capacity mix of the power plant at different minimum baseload ( $BL_{min}$ ) scenarios and a hydrogen price of 4 €/kg

The wind farm capacity is fixed at 5 GW due to the project requirements (and therefore not displayed in the charts) and in the GFB parts, variations can be seen with similar trends observed based on the increasing  $BL_{min}$  scenarios regardless of the hydrogen price. In scenarios with constant baseload such as  $BL_{min}$  10/10%, 15/15%, and 20/20%, no investment is done for the OCGT while in flexible baseload scenarios (meaning there is a difference between summer and winter), a relatively small investment in OCGT is seen. This indicates that for most of the year, the minimum baseload requirement is fulfilled by the CCGT and there are only a few hours per year where an additional generation capacity that can be fulfilled by a peak technology such as OCGT is required. Furthermore, in scenarios where the model invests in reconversion technologies, the sum of the capacities is always equal

to the maximum  $BL_{min}$  requirement since the power plant must ensure the supply of that amount of electricity at all times, including on hours with zero wind generation, i.e. fulfilling the role of a baseload supplier.

As mentioned previously, hydrogen price and  $BL_{min}$  requirements dictate the size of the electrolyzer, storage, and reconversion technologies. As seen in Figures 4.6, 4.7, and 4.8, higher hydrogen prices for the same  $BL_{min}$  cases see a higher capacity investment in the electrolyzer but lower in storage while the size of the CCGT and OCGT stays the same between hydrogen prices. The reconversion technology remains the same since the value of selling electricity from the GFB section to the grid has a lower economical value than selling hydrogen to industry, and in order to maximize profit the model prefers not to invest in more capacity than the required to satisfy  $BL_{min,winter}$ . The storage size and electrolyzer size variations are related to the operation of said components. With higher price of hydrogen, the model invests in less storage since the value of reconverting hydrogen to electricity during high electricity price hours does not add significant profit considering the revenue made by selling hydrogen to industry, therefore the GT will operate to cover the minimum baseload and during some few extra hours. The electrolyzer capacity increases with hydrogen price since its costs are covered by the increased revenue, and although the yearly demand is fixed, the hourly demand is not, and the model optimizes the generation of hydrogen at each timestep.

In addition, increasing  $BL_{min}$  requirements means increasing the sizes of all the GFB components. This means that the primary driving factor in determining the size of the GFB components is the  $BL_{min}$  requirements. The maximum  $BL_{min}$ , i.e. the  $BL_{min,winter}$  determines the sizes of the reconversion technologies, which in turn affects the additional storage capacity to fuel the reconversion on top of the prevailing industry hydrogen demand, and lastly the electrolyzer needed to provide the hydrogen. Therefore, the reason for decreasing profitability for higher  $BL_{min}$  cases is due to the fact that it requires an increased amount of investment in the GFB components (electrolyzer, storage and reconversion technology) as seen in Figures 4.6, 4.7, and 4.8. Since profit is defined as revenue minus the annualized investment cost and the sum of both fixed and variable operation and maintenance costs of the GFB components, designs with higher maximum  $BL_{min}$  tend to have lower profitability due to the cost element.

When studying the design for each of these cases, it is important to consider that these designs have been optimized for a five-year period since individual years have different wind productions, and thus, yielding different results. When running the model for individual years, the results are different, both between each other and with the five-year period. To further clarify this, one of the cases was chosen:

## 4. Results

$BL_{min,summer} = 10\%$  and  $BL_{min,winter} = 20\%$  and  $price^{industry} = 4\text{€}/\text{kg}$  and  $BL_{max}$  of 72%. Figure 4.9 displays an example of different designs obtained when running the chosen case for individual years.

All of the cases have a fixed wind farm capacity of 5 GW and therefore the WF capacity is not included in the chart in Figure 4.9. From the figure, it can be seen that under different wind profiles and electricity price years, the capacity mixes determined by the model are different. Moreover, the distribution of CCGT and OCGT capacity investment varies depending on the year being simulated even though the total installed capacity of the gas turbines remained constant according to the  $BL_{min,winter}$ , i.e. 1 GW. This is because, in some years, the amount of high-price hours is not enough to justify the additional investment in CCGT capacity, and therefore an investment in OCGT that can be ramped up as needed is preferred in those cases.



**Figure 4.9:** Capacity mix of the GFB components with BLmin 10/20% at 5 different year scenarios and a hydrogen price of 4 €/kg. (a. Electrolyzer, CCGT, and OCGT capacities. b. Storage capacity)

As seen from Figure 4.9, the variations in storage investment are quite significant, with a difference of almost 125 GWh between the years 2010 and 2019. According to Figure 2.4, 2010 is a year of very low wind in comparison with the others, which explains the larger investment in storage, since a minimum supply of electricity must be guaranteed throughout the whole year.

### 4.2.1 LCOE analysis of Scenario 2

The effects of the various  $BL_{min}$  combinations on the LCOE in this scenario were calculated to find out how the addition of reconversion technologies caused by the enforced minimum baseload impacts the LCOE and the results are displayed in Tables 4.2, 4.3, and 4.4. Each of the tables shows the LCOE of the wind farm component ( $LCOE_{WF}$ ), the GFB part with the revenue of hydrogen both included and not included ( $LCOE_{GFB,H2}$  and  $LCOE_{GFB,0}$ , respectively), and the entire power plant with the revenue of hydrogen to the industry included ( $LCOE_{PP,H2}$ ) and not included ( $LCOE_{PP,0}$ ).

**Table 4.2:** LCOE analysis of different  $BL_{min}$  combinations in Scenario 2 at a hydrogen price of 2.4 €/kg, for  $BL_{max} = 72\%$ .

Hydrogen price 2.4 €/kg	$LCOE_{WF}$ [€/MWh]	$LCOE_{GFB,0}$ [€/MWh]	$LCOE_{GFB,H2}$ [€/MWh]	$LCOE_{PP,0}$ [€/MWh]	$LCOE_{PP,H2}$ [€/MWh]
<b>BLmin 10/10%</b>	54,98	231,37	186,30	62,07	60,26
<b>BLmin 10/15%</b>	55,93	220,63	173,47	64,76	62,23
<b>BLmin 10/20%</b>	58,00	215,42	167,57	69,13	65,75
<b>BLmin 15/15%</b>	57,60	186,78	143,13	67,24	63,98
<b>BLmin 15/20%</b>	59,11	183,39	138,53	70,41	66,33
<b>BLmin 20/20%</b>	63,19	175,38	132,50	76,83	71,62

**Table 4.3:** LCOE analysis of Scenario 2 at a hydrogen price of 3 €/kg, for  $BL_{max} = 72\%$ .

Hydrogen price 3 €/kg	$LCOE_{WF}$ [€/MWh]	$LCOE_{GFB,0}$ [€/MWh]	$LCOE_{GFB,H2}$ [€/MWh]	$LCOE_{PP,0}$ [€/MWh]	$LCOE_{PP,H2}$ [€/MWh]
<b>BLmin 10% to 10%</b>	55,03	236,58	191,49	62,35	60,54
<b>BLmin 10/15%</b>	56,06	225,28	178,05	65,17	62,63
<b>BLmin 10/20%</b>	57,58	216,75	168,61	68,79	65,40
<b>BLmin 15/15%</b>	57,86	187,41	143,71	67,58	64,30
<b>BLmin 15/20%</b>	59,67	185,56	140,81	71,22	67,11
<b>BLmin 20/20%</b>	63,53	177,46	134,72	77,38	72,18

**Table 4.4:** LCOE analysis of Scenario 2 at a hydrogen price of 4 €/kg, for  $BL_{max} = 72\%$ .

Hydrogen price 4 €/kg	$LCOE_{WF}$ [€/MWh]	$LCOE_{GFB,0}$ [€/MWh]	$LCOE_{GFB,H2}$ [€/MWh]	$LCOE_{PP,0}$ [€/MWh]	$LCOE_{PP,H2}$ [€/MWh]
<b>BLmin 10/10%</b>	55,04	236,58	191,49	62,37	60,55
<b>BLmin 10/15%</b>	56,18	227,15	179,85	65,43	62,87
<b>BLmin 10/20%</b>	57,85	219,76	171,51	69,32	65,90
<b>BLmin 15/15%</b>	58,04	188,73	145,26	67,85	64,59
<b>BLmin 15/20%</b>	60,18	189,03	144,16	72,11	67,96
<b>BLmin 20/20%</b>	64,22	178,64	135,87	78,37	73,09

When compared to each other, Tables 4.2, 4.3, and 4.4 show that the LCOE varies slightly with the difference in hydrogen prices, with a higher LCOE for higher hydrogen prices. This is due to the fact that the price of hydrogen impacts the capacity mix from the model (and therefore the investment and O&M costs). In turn, it affects how the components operate throughout the year and subsequently the LCOE of the different parts of the WF, GFB, and the entire power plant (PP).

Another trend that can be observed from the LCOE calculations is that higher  $BL_{min}$  scenarios increase the LCOE of the WF and PP, but decreases the LCOE of the entire GFB. This result comes from the fact that in higher  $BL_{min}$  scenarios, there is more electricity supplied by the GFB component due to the enforced minimum baseload throughout the year. As LCOE is defined by the cost of the components related to electricity production divided by the amount of electricity produced and sold, this naturally lowers along with a higher amount of electricity produced as the denominator.

## 4.2.2 Operation of designs

In this section, a description of the operation of the power plant as a whole will be provided to better understand the role of each component and the added value of the GFB to the system. For this analysis, the case of  $BL_{min,summer} = 10\%$  and  $BL_{min,winter} = 20\%$  is chosen for the explanation of these results.

Figure 4.10 displays the wind profile load duration curve for the five-year period being studied. It can be seen that the wind electricity supplied to grid is significantly smaller than the total produced electricity, meaning that it is either being curtailed or used in the electrolyzer. When there is insufficient wind (rightmost side of the figure), the gas turbine is ramped up to supply the minimum baseload required.

It is of interest to note that there are some hours where, regardless of wind pro-

duction being sufficient to cover the minimum baseload, the gas turbine supplies electricity to the grid anyways (see middle section of the figure). This is due to high electricity prices being present at these hours, giving a large economic value to the electricity sold and thus the gas turbine is ramped up. Another observation that can be withdrawn from Figure 4.10 is the energy loss throughout the hydrogen production and reconversion process. The area below the wind production curve (red line), indicates electricity produced by the wind farm. The blue area represents the actual electricity being supplied to the grid from the wind farm. Therefore, the empty area between the red line and the blue area represents electricity generated by the wind farm which is either being fed to the electrolyzer or curtailed. The green area represents the electricity generated by the gas turbine. Due to hydrogen demand from the industry, this area is significantly smaller than the white space under the red line (electricity generated by the wind farm but not being supplied to the grid), since some of the wind-generated electricity is used in the electrolyzer to fulfill the demand from the industry. To a lesser extent, part of this reduction in area is also related to the efficiency losses associated with the production of hydrogen, its storage, and the later reconversion.

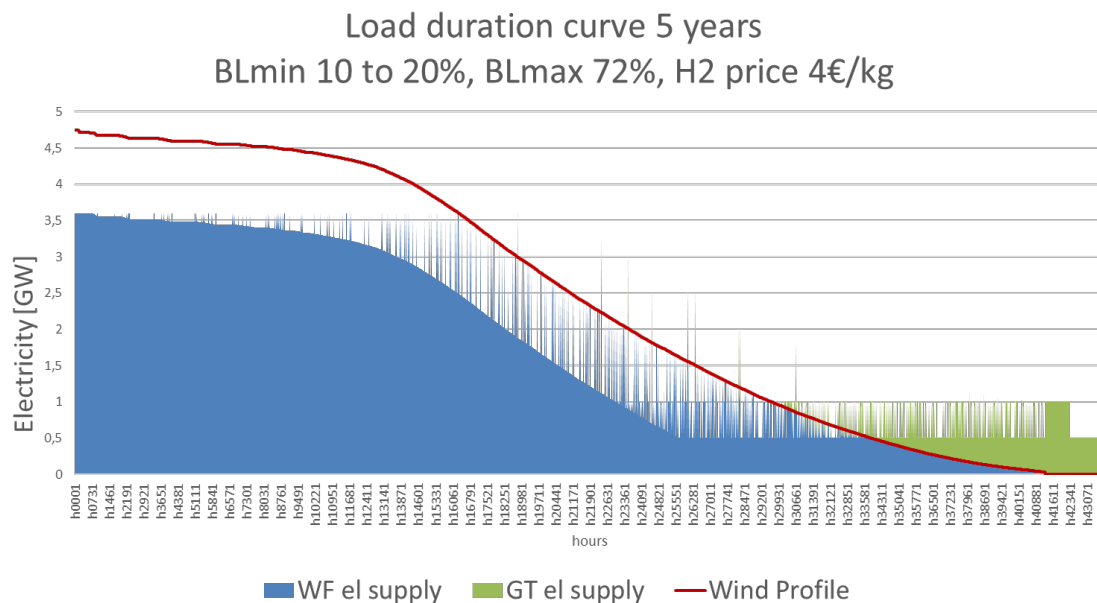


**Figure 4.10:** 5-year period load duration curve of the power plant operation with BLmin 10/20%, BLmax = 72% and hydrogen price of 4 €/kg.

As observed in Figure 4.11, there are two plateaus in the minimum supply to electricity, at 10% (0.5GW) and 20% (1GW). These correspond to 22.4% and 17.8% of the total five-year period, respectively. In this flexible baseload case, the gas turbine supplies the full minimum baseload requirement during 3.4% of the time

## 4. Results

$BL_{min} = 10\%$  is required, and 2.4% of the time  $BL_{min} = 20\%$  is needed. For this combination of  $BL_{min}$ , it is interesting to highlight the utilization of the maximum grid capacity,  $BL_{max} = 72\%$  or 3.6GW. In this case, the maximum grid capacity is used during 5.1% of the time. Additionally, 90% of this maximum connection (i.e. 3.24GW) is used during 28.2% of the hours. This indicates that the maximum grid connection is being used for quite a significant period of time, but that the most optimal  $BL_{max}$  should be investigated further, as there can exist a most optimal capacity of grid connection.

For this combination of  $BL_{min}$ , it is interesting to highlight the utilization of the maximum grid capacity,  $BL_{max} = 72\%$  or 3.6GW. In this case, the maximum grid capacity is used during 5.1% of the time. Regardless, 90% of this maximum connection (i.e. 3.24GW) is used during 28.2% of the hours. This indicates that the maximum grid connection is being used for quite a significant period of time, but that the most optimal  $BL_{max}$  should be investigated further, as there can exist a more optimal capacity of grid connection.

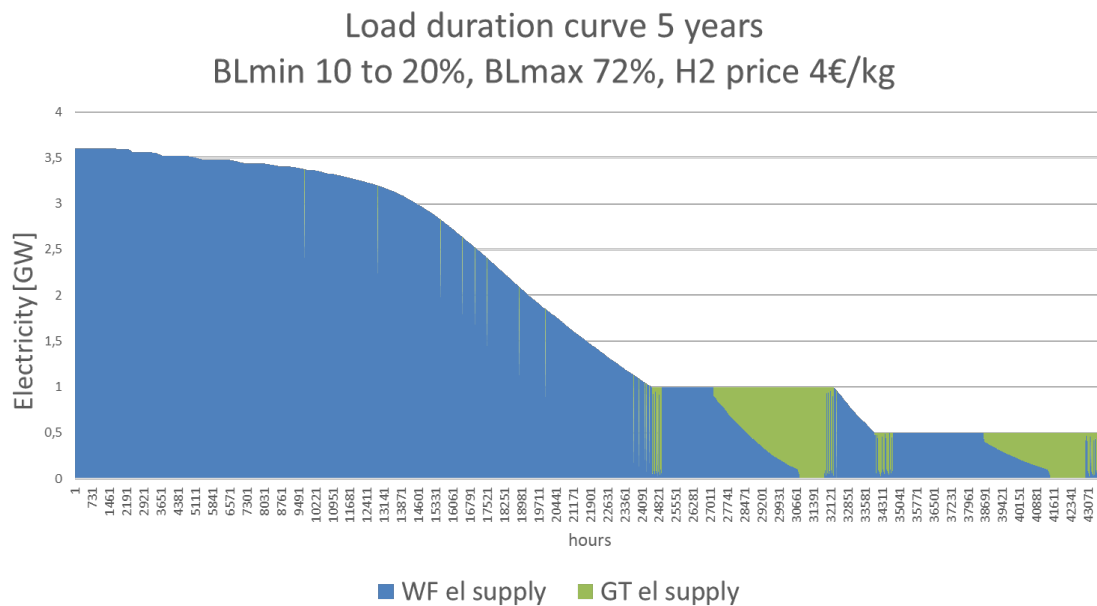


**Figure 4.11:** 5 year period load duration curve of the power plant operation with  $BL_{min} 10/20\%$ ,  $BL_{max} = 72\%$  and hydrogen price of 4 €/kg.

In order to better understand the hourly operation of the different components of the power plant, a yearly analysis of the results is provided (Figure 4.12.). The chosen year for this analysis is 2016, which corresponds to the middle point in the selected five-year period, and it is the year that happens to lie between the most and least windy profiles used in this simulation, according to Figure 2.4.

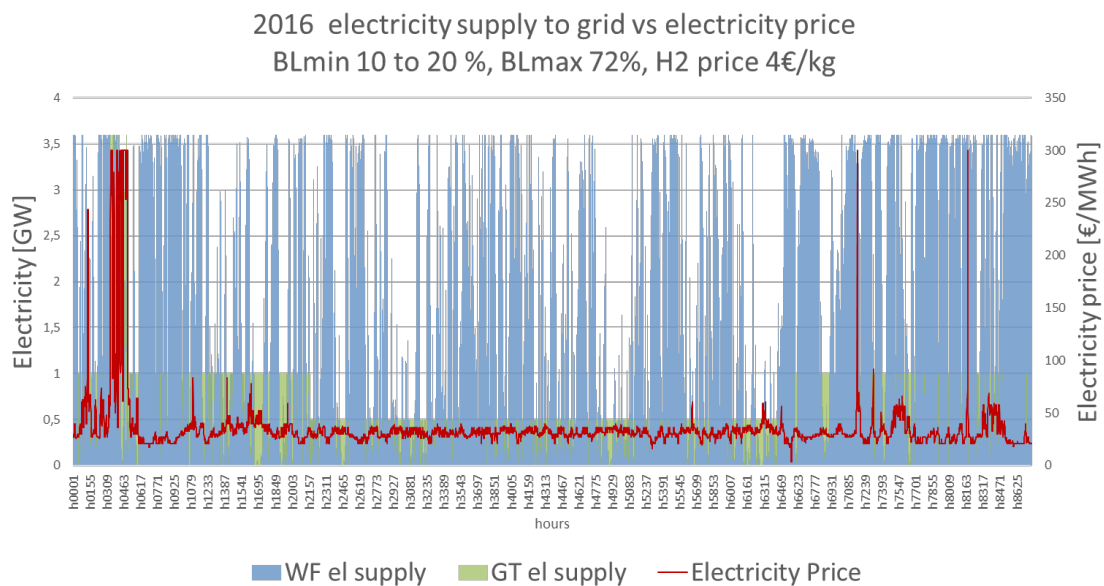


**Figure 4.12:** Yearly electricity supply of the power plant for 2016 with BLmin 10/20%, BLmax = 72% and hydrogen price of 4 €/kg.

From the figure above, the variability of wind production can be appreciated, as well as the peaks in electricity prices that are experienced mainly during the winter periods. It also clearly shows the role of the gas turbine as a complementary technology in the system in order to provide the minimum selected baseload. The figure also clearly highlights the difference in electricity prices between summer and winter, where in the middle section (summer), the prices are more constant and generally lower, whereas the high peaks in prices are experienced throughout the winter months.

In order to better understand the hourly operation of these plants, a summer month and a winter month were selected: July and January, respectively. Figure 4.13 shows the electricity supply of the power plant in July 2016. The multi-day variability of wind generation is visible in Figure 4.13, with larger wind production at the beginning of the month than at the end. The prices this month are quite low (around 40 €/MWh being the maximum), therefore the economic value of reconverting hydrogen into electricity is not as high as that of selling hydrogen. Thus, only the enforced minimum baseload is being supplied when the wind farm does not generate sufficient electricity. Some differences can be appreciated from the figures. Around the third period of high wind (i.e., the third cluster of tall blue columns), it can be seen that for this constant baseload case, there is a lower supply of electricity from the wind farm to the grid. This means that this electricity is instead being used in the electrolyzer, as in this constant baseload case, the minimum supply is higher (15%) than for the flexible case (10%) and therefore requires a larger hydrogen production

## 4. Results

in the studied month.

The behavior of the power plant is different throughout the winter, therefore the electricity supply during January 2016 is displayed in Figure 4.14.

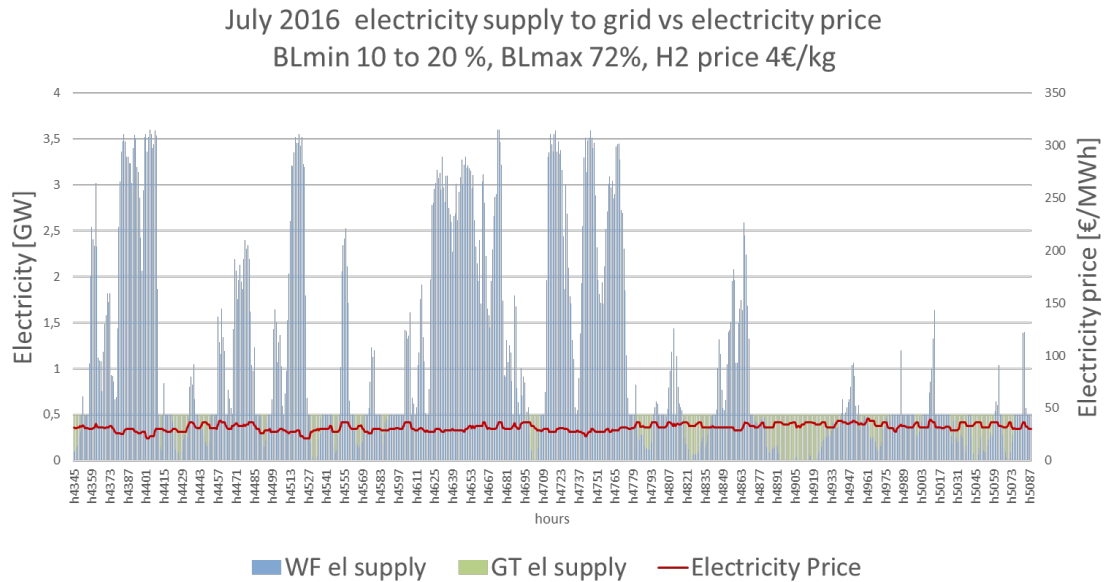


**Figure 4.13:** Electricity supply of the power plant for July 2016 with BLmin 10/20%, BLmax = 72% and hydrogen price of 4 €/kg.

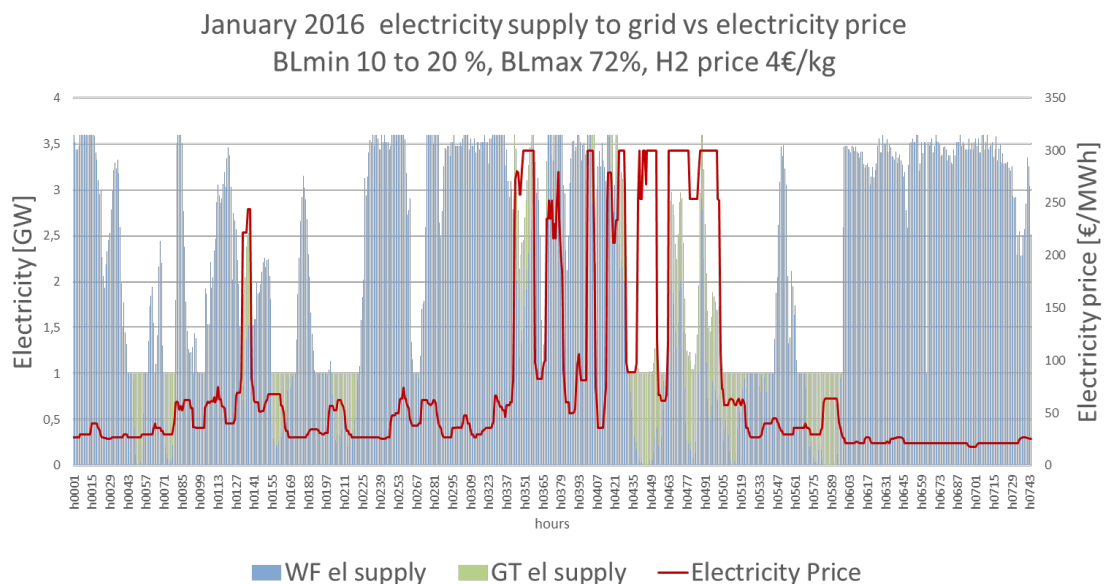


**Figure 4.14:** Electricity supply of the power plant for January 2016 with BLmin 10% to 20%, BLmax = 72% and hydrogen price of 4 €/kg.

One of the most important observations that can be made from Figures 4.13 and 4.14

is the supply of electricity from the gas turbine. Both cases display multiple hours at which there is sufficient wind-generated electricity to supply to the grid, but since the price reaches high values (even the maximum of 300 €/MWh), the gas turbine generates electricity also above the  $BL_{min}$ . This means that the added economic value of reconverting hydrogen to electricity is sufficiently large to compensate for the costs and therefore additional electricity is generated in the gas turbine.

Another observation that can be made is how the wind also varies throughout the winter in multiple-day periods, but how overall the amount of wind is larger than that during the summer. This also explains why the gas turbines are running even if the minimum baseload is met because the hydrogen production is large enough to be supplied to the industry and to fuel the turbines.

The GFB section of the power plant is the one managing internally its variations and therefore an evaluation into the operation of its single components was carried out. Figures 4.15 and 4.16 display the hourly storage level and hydrogen production, and the hydrogen usage, respectively. These figures can be compared also with Figure 4.14 to better understand how the wind production affects the GFB section.

From comparing Figures 4.15 and 4.16, it can be seen that at no point do the gas turbine and the electrolyzer operate at the same time, i.e. hydrogen cannot be used as a fuel at the same time as it is being produced. In high electricity-price hours, the production of hydrogen is stopped, and the supply to industry lowered so that the hydrogen can instead be used to produce electricity in the gas turbine (see middle part of Figure 4.16). It can also be observed that when the electricity prices are lower, the hydrogen supply to industry is increased, since there is less incentive to sell to grid and the main goal is to maximize the profit of the plant.

Figures 4.15 and 4.16 show how the hydrogen production, storage, and utilization operate. In this instance, the minimum baseload for the winter is 20%, thus demanding more hydrogen than the during the summer months. This can be observed in the smaller supply of hydrogen to the industry (4.16), where it is seen that the supply of hydrogen to industry during this month is mostly in the lower limit of the hourly flexible supply, since it has to be used to ensure the supply of the minimum baseload (1GW). The right-hand side of Figures 4.15 and 4.16 corresponds to a high wind period, and therefore the GT does not have to operate to cover the minimum baseload. During this period, the electrolyzer is run at full capacity to fill up the storage, to ensure there is enough hydrogen to cover the next instances of low wind.

## 4. Results

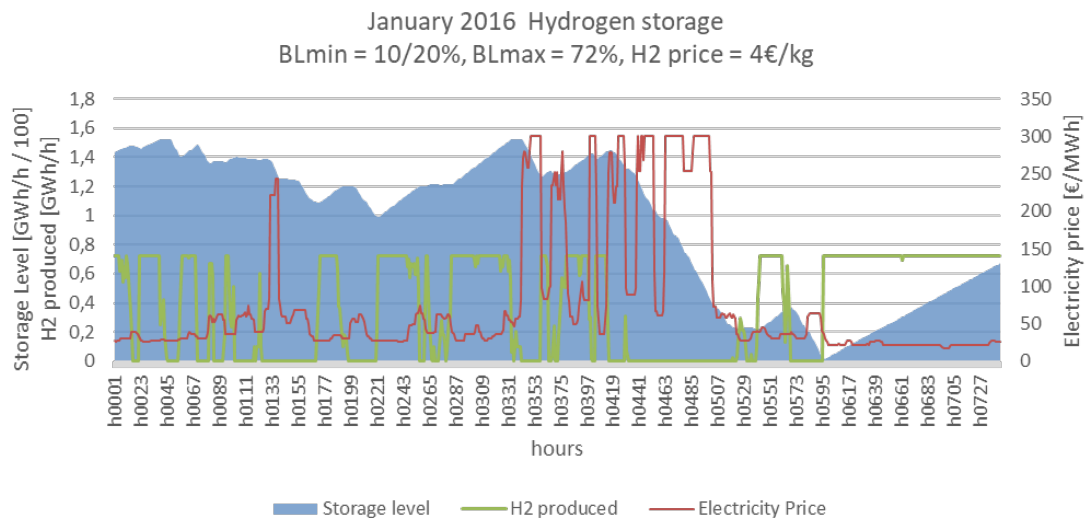


**Figure 4.15:** Hydrogen storage level, hydrogen production in the electrolyzer and electricity prices for January 2016 with BLmin 10/20%, BLmax = 72% and hydrogen price of 4 €/kg.

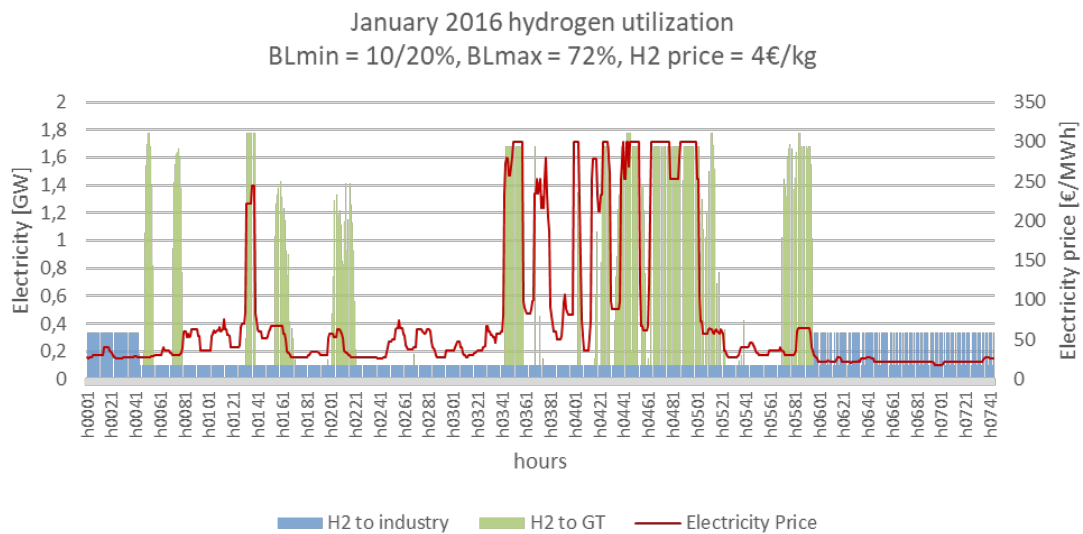


**Figure 4.16:** Hydrogen utilization in the gas turbines and supply to industry for January 2016 with BLmin 10/20%, BLmax = 72% and hydrogen price of 4 €/kg.

### 4.2.3 Robustness analysis of designs

After running the model with multi-year data and obtaining the optimal capacity mix for different minimum baseload scenarios, two final designs were chosen for further analysis. The designs chosen are  $BL_{min}$  10% to 20% and  $BL_{min}$  15% to 15%. For this analysis, the chosen  $BL_{min}$  combinations were selected to stay closer

to the original proposal (constant minimum supply), and to be able to supply the highest  $BL_{min}$  analyzed ( $BL_{min} = 20\%$ ). The goal of this analysis was to verify the designs selected by the model for a five-year period for separate years, with the aim of analyzing the robustness and profitability of the chosen capacities.

In this analysis, the simulations are based on 72% grid connection ( $BL_{max}$ ) and a hydrogen price of 4 €/kg. The capacity mixes for the chosen cases ( $BL_{min}$  10% to 20% and  $BL_{min}$  15% to 15%) was used as input for the model to run for the years 2010, 2016, and 2018. The results were sorted and plotted to form a load duration curve shown in Figures 4.17 and 4.18.

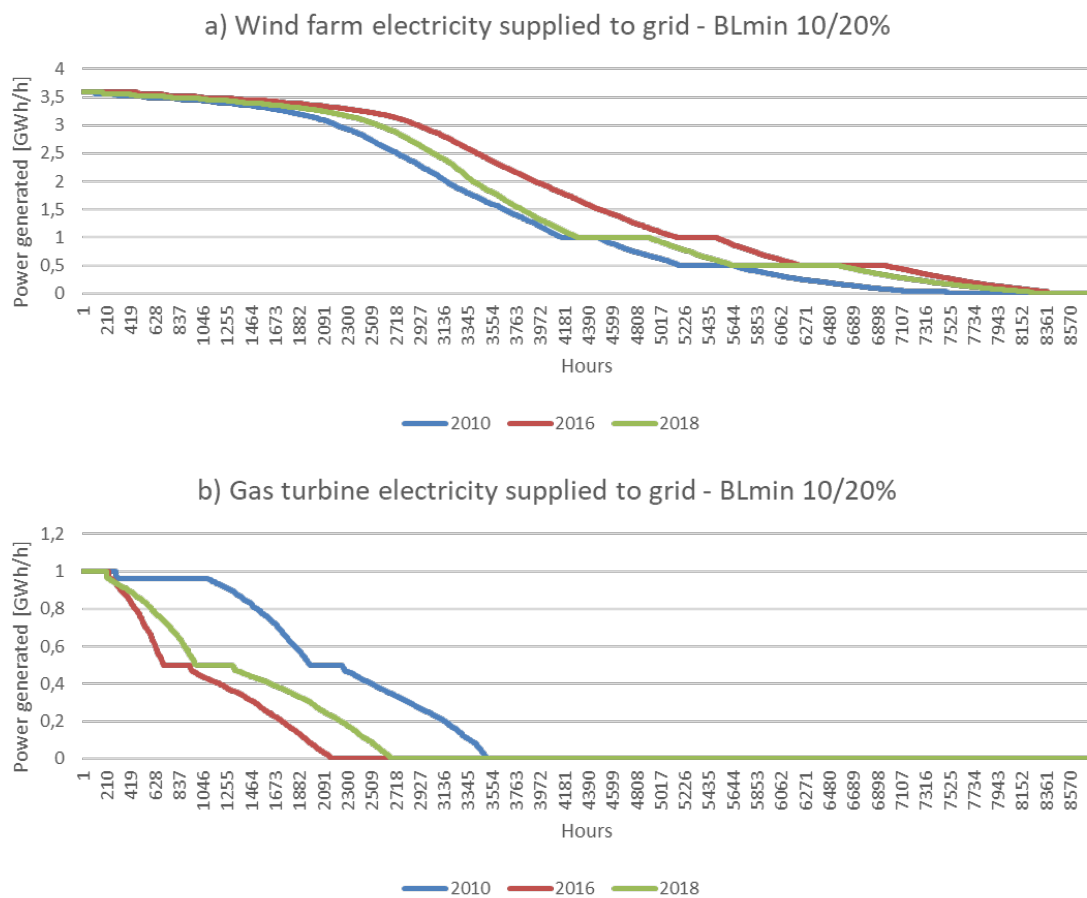


**Figure 4.17:** Load duration curve of the power plant operation with BLmin 10/20% with 3 different year scenarios and a hydrogen price of 4 €/kg

Figures 4.17 and 4.18 show that overall, the yearly load duration curves are similar to each other for the same  $BL_{min}$  cases with a difference in the number of hours they are operating at a certain capacity. The gas turbines operate more hours and with a higher capacity to compensate during the year with lower amounts of wind (2010) compared to years with more wind (2016 and 2018) (refer to Figure 2.4 for

## 4. Results

the different wind profile load duration curves). Between the different minimum baseload cases, there is also a visible difference in how the gas turbine operates where in Figure 4.17, there are 2 plateaus in the load duration curve of the electricity supplied to the grid by the gas turbine corresponding to the two different levels of  $BL_{min}$  whereas there is only one for the constant minimum baseload case.

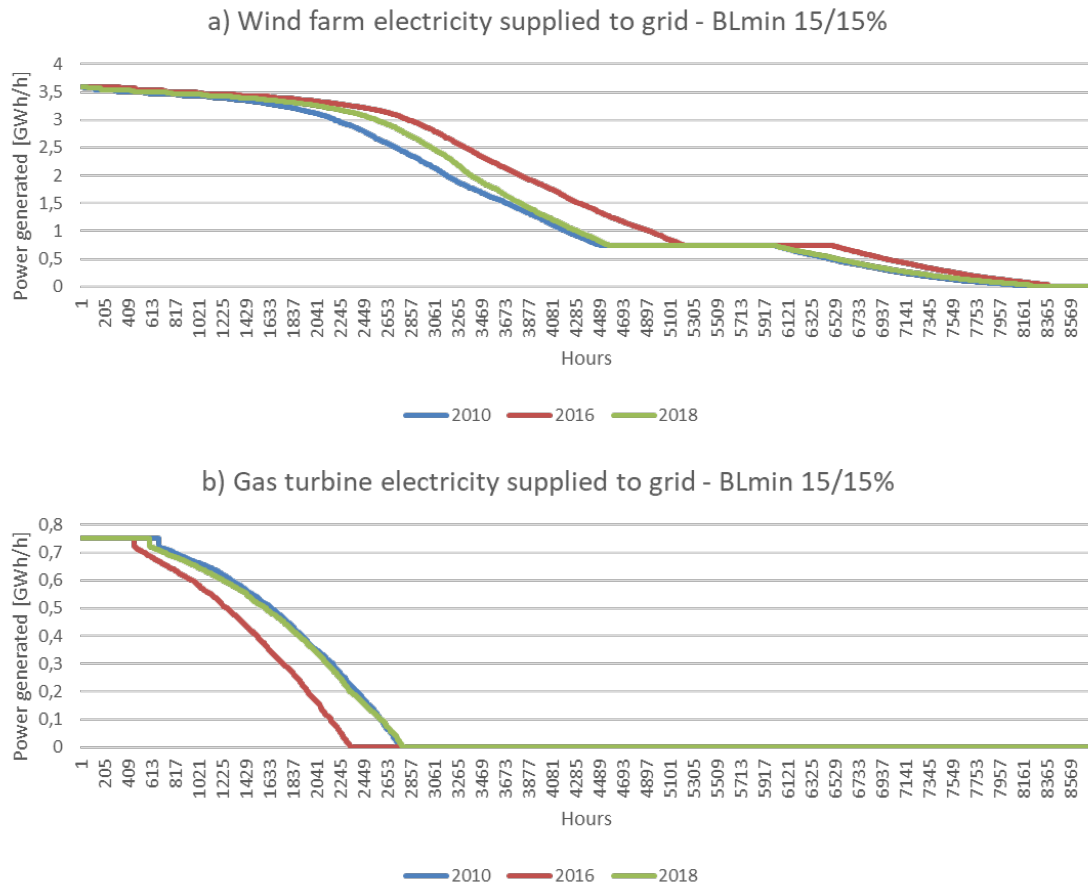


**Figure 4.18:** Load duration curve of the power plant operation with  $BL_{min}$  15/15% with 3 different year scenarios and a hydrogen price of 4 €/kg

Table 4.5 shows the profit of the power plant and parts of the profit that come from the GFB part of the power plant in the 3 simulated years. This analysis was done to show that the operation of the power plant and the profits can vary between each year in operation depending on the weather and the electricity prices, which will be further discussed in the next chapter. As seen from the table, the designs are profitable almost every year, with the lowest profit made on year 1, which corresponds to a low wind year, 2010, as seen from Figure 2.4. This is expected, since having a forced  $BL_{min}$  during a low wind year means that part of the electricity that could be sold from the wind farm to the grid must be diverted to the electrolyzer to generate enough hydrogen to be able to fulfill this constraint.

**Table 4.5:** Yearly profit breakdown of the power plant with  $BL_{min}$  10% to 20% and  $BL_{min}$  15% to 15% cases.

Profit GFB [M€]	2010	2016	2018
$BL_{min} = 10\%$ to $20\%$	-25,06	65,28	39,67
$BL_{min} = 15\%$ to $15\%$	48,41	88,09	54,04

This analysis shows the fact that the chosen capacities for the five-year simulation has varying levels of profitability when seen on a yearly basis with some years operating on losses and others being profitable. Nevertheless, it results in overall profit in the long run (i.e. five years in the case of this project).



# 5

## Discussion

This chapter aims to discuss the results displayed in Chapter 4 - how the results have been affected by the different methodological assumptions carried out and what are the consequences of the obtained results. Also, an answer to the posed questions of Section 1.3 will be sought.

The analysis performed in Chapter 4 allowed for a better understanding of how the feasibility of the GFB plant is affected. Three main factors can be highlighted from the results: the hydrogen price to the industry, the maximum grid connection capacity  $BL_{max}$ , and the imposed minimum baseload requirement  $BL_{min}$ . Firstly, the hydrogen price plays a major role, since hydrogen to industry is the largest revenue inflow of the GFB. This implies, that for profit maximization, the sale of hydrogen has the most significant contribution. This can be clearly observed from the results in Section 4.1, where when given full freedom to invest or not in GT ( $BL_{min} = 0\%$ ) the model chooses to behave solely as a hydrogen producer.

According to the assumptions made in Section 3.2, the hydrogen price was chosen to be within the conservative side of the predicted prices in the future. It is important to consider that if hydrogen prices are higher in the future, it will benefit the economic feasibility of the GFB, as a larger profit would be made from it. But it is also important to account for the fact that prices will most likely fluctuate, and therefore so will the revenue stream of the GFB. Another factor affecting the revenue from hydrogen is the demand of the industry, which in the present analysis was set to be constant each year, but with a flexible hourly supply (refer to Section 3.2). This assumption depends on the future behaviour of the industry, and the flexibility which an industry is willing to accept in the supply. These aspects were not investigated further in the model since they were out of the scope, but these could largely affect the profitability of the power plant.

Besides the price of hydrogen being a main determinant in the economic feasibility of the power plant, it was also seen that the connection capacity to grid plays a major role (as observed in Figures 4.2 and 4.3). The costs reductions available from

a reduced grid connection affect the overall profitability of the power plant as the wind farm costs are lowered. When imposing a baseload minimum it was seen that the profit made from selling electricity at larger than 72% connection to grid is not large enough to compensate the cost.

Lastly, it was determined that the imposed baseload minimum plays a major role in the profitability of the GFB, as seen from the results evaluated in Figure 4.4. As mentioned before, if no  $BL_{min}$  is enforced, the model simply behaves as a hydrogen producer as it is the most profitable design. Therefore, imposing a minimum baseload decreases the profitability of the plant. Since  $BL_{min,winter}$  is the determining factor for the investments made in reconversion technologies, which in turn determine the needed capacity from the electrolyzer and storage, the larger the  $BL_{min,winter}$  the lower the profitability of the power plant (as seen in Figure 4.4).

An important goal of this project was to determine the design of the GFB power plant for it to be profitable under the many design constraints imposed. During Section 4, multiple designs have been proposed for the five-year period analyzed. After evaluating the results obtained and the profitability of these designs, it can be discussed that multiple options exist which make the power plant profitable. Although the LCOE of the plants analyzed in Scenario 2 is higher than the case for the wind only scenario, it was decided that the value of supplying a baseload to the grid behaving as a VMS, gives the power plant a value that is not economical in nature. The chosen suggested as a result of this project is  $BL_{min,summer} = 10\%$ ,  $BL_{min,winter} = 20\%$  and  $BL_{max} = 72\%$ . This was decided since the plant is profitable and the minimum baseload supplied is quite large (1 GW) in the winter.

When analyzing the chosen design, it is important to consider that the model behaves reacting to a total overview of the five-year period. In reality, there is no knowledge of the future hourly wind power profiles and electricity prices, and therefore the design chosen will behave differently than the results obtained. It was believed that by implementing a larger  $BL_{min,winter}$  extra operational flexibility is available for the design. The installed capacity of the reconversion technology is 1 GW, so in the event that the future prices and wind profiles behave differently from what was assumed in this project, the plant has more flexibility and can operate at a wider range of capacity than if the imposed minimum baseload was lower.

Another goal of the project was to determine the operation of the chosen designs. As hypothesised, part of the electricity generated by the wind farm during high wind periods of time and low electricity prices is supplied to the electrolyzer to generate hydrogen to sell to industry or reconvert to electricity accordingly. The hydrogen is reconverted to electricity to fulfill the minimum baseload enforced, but gas turbines are also ramped up during periods of electricity prices spikes (as shown in Section

4.2.2). The analysis on the behaviour of the power plant could be further expanded if the effects of the power plant on the electricity system itself were taken into account. As the model is design currently, the electricity prices are fixed and the power plant reacts accordingly to maximize the profit made. In reality, due to the large size of the wind farm being installed, it could be discussed that it will have an effect on the electricity system and most importantly in the electricity prices. This two-way interaction of the power plant with the system would most likely affect the obtained design results and their operation.

It can also be argued that the results obtained throughout this project are also affected by the data used and the demands specified. For example, the chosen time period was five years in order to account for the inter-year variability of wind. In order to obtain a more generalized design that can operate with different wind profiles, it would be beneficial to run the model for longer periods of time. Additionally, there are several uncertainties that cannot be captured and modeled perfectly such as the effects of climate change on future weather which might have an effect on how the wind profile looks in the future and in turn, the operation of the wind farm itself.

All in all, when considering the model developed and the obtained results, it can be determined that the proposed project of a GFB power plant has a potential value in the system, from the VMS perspective, and can also become a profitable investment. The chosen design of  $BL_{min,summer} = 10\%$ ,  $BL_{min,winter} = 20\%$  and  $BL_{max} = 72\%$  can be a viable option in the near future, managing wind power variations while maximizing its profit. It can be discussed that such a power plant could become competitive against other baseload suppliers such as nuclear, since when comparing the latter's LCOE ( $LCOE = 81\text{€}/MWh$  [50]) to the LCOE of the chosen design,  $LCOE_{PP} = 65.9\text{€}/Mwh$ , it is significantly larger.

## 5.1 Future work

After carrying out the modeling and evaluation of the GFB power plant, it was determined that the work carried out could be further improved and so some future work is suggested to continue this project.

First, as mentioned previously in this chapter, it would be of great interest to evaluate the effect of such a power plant on the electricity system. Instead of letting the model accept given electricity prices, it would be most interesting to connect it to a more complete model of the system and the effect that this plant has on the prices be evaluated. It is expected that this would result in different chosen design for the different components and different operation of the latter.

Additionally, the scope of this project was reduced to the Swedish electricity system. Since the presence of hydro power in the electricity mix is so large, and this technology is quite flexible in its operation, the electricity prices are largely affected by the operation of hydro power. It would be interesting to analyze the behavior of this power plant in a different electricity system where hydro power does not play such an important role (i.e. UK).

Furthermore, the analysis performed throughout this thesis only included five specific weather years and corresponding electricity prices. In order to further generalize the results and evaluate the operation and profitability of the GFB power plant in other scenarios, a larger range of years is suggested for the analysis.

Lastly, the analysis on the optimal  $BL_{max}$  was reduced to only three different grid connections ( $BL_{max} = 44, 72, \text{ and } 100\%$ ). It is expected that there is a most optimal connection point and thus a sensitivity analysis is recommended to determine which grid connection is the most beneficial economically for the GFB power plant.

# 6

## Conclusion

This thesis discusses the techno-economical analysis of an offshore wind farm combined with hydrogen production, storage, and reconversion as a Green Flexible Baseload (GFB) concept, to be operated in southern Sweden in 2030. The analysis performed was focused on the maximization of profit made by the wind power plant when acting as an electricity generator and hydrogen supplier. Assumptions of future electricity and hydrogen prices, and components' and fuels' costs were made for the future time-frame considered in this thesis. Weather data from the south of Sweden was used to determine wind power production and predict future electricity prices.

It was determined that the factors which affect the economical feasibility of the power plant are the hydrogen price to industry, the maximum grid connection, and the minimum baseload requirement. The larger the hydrogen prices the larger the profit made by the power plant. A most optimal grid connection capacity was determined for the different scenarios studied, being 100% when no  $BL_{min}$  is imposed, and 72% for the cases with a set  $BL_{min}$ . Lastly, as explained in Chapters 4 and 5,  $BL_{min,winter}$  is the main determinant of the capacities of the GFB section, and thus the larger it is, the higher the investments, and the lower the profit.

It was concluded that there are multiple design combinations that result in profit without the requirement of subsidies. Two designs are suggested as profitable options in a scenario where hydrogen price is 4€/kg: a constant  $BL_{min} = 15\%$  design with  $BL_{max} = 72\%$ ; and a flexible minimum baseload  $BL_{min,summer} = 10\%$  and  $BL_{min,winter} = 20\%$  with  $BL_{max} = 72\%$  are proposed. The capacity of the different components can be found in Table B.3 in Appendix B.

The wind power variations can be managed within the power plant when the GFB section is added to it, which could significantly benefit a future electricity system highly penetrated by VRE. The effect of such a power plant on the electricity mix and prices is suggested as future work to better understand the role of such technology as a VMS.



# Bibliography

- [1] *Goals archive*. [Online]. Available: <https://www.globalgoals.org/goals/>.
- [2] Iea, *Outlook for electricity – world energy outlook 2022 – analysis*. [Online]. Available: <https://www.iea.org/reports/world-energy-outlook-2022/outlook-for-electricity>.
- [3] H. Ritchie, M. Roser, and P. Rosado, “Co2 and greenhouse gas emissions,” *Our World in Data*, 2020. [Online]. Available: <https://ourworldindata.org/co2-and-greenhouse-gas-emissions>.
- [4] [Online]. Available: [https://commission.europa.eu/strategy-and-policy/priorities-2019-2024/european-green-deal\\_en](https://commission.europa.eu/strategy-and-policy/priorities-2019-2024/european-green-deal_en).
- [5] [Online]. Available: <https://www.epa.gov/ghgemissions/global-greenhouse-gas-emissions-data>.
- [6] J. Jaeger, *Explaining the exponential growth of renewable energy*, Sep. 2021. [Online]. Available: <https://www.wri.org/insights/growth-renewable-energy-sector-explained>.
- [7] IEA. “Renewable electricity.” (2022), [Online]. Available: <https://www.iea.org/reports/renewable-electricity>.
- [8] V. Walter, “Cost-efficient integration of variable renewable electricity variation management and strategic localisation of new demand,” Ph.D. dissertation, Department of Space, Earth and Environment CHALMERS UNIVERSITY OF TECHNOLOGY, 2022.
- [9] P. D. Lund, J. Lindgren, J. Mikkola, and J. Salpakari, “Review of energy system flexibility measures to enable high levels of variable renewable electricity,” *Renewable and Sustainable Energy Reviews*, vol. 45, pp. 785–807, 2015. DOI: <https://doi.org/10.1016/j.rser.2015.01.057>. [Online]. Available: <https://www.sciencedirect.com/science/article/pii/S1364032115000672>.
- [10] *International cooperation*, Mar. 2021. [Online]. Available: <https://www.svk.se/en/national-grid/operations-and-electricity-markets/international-cooperation/>.

- [11] K. Bjerndal, *Minskad elanvändning under 2022*, Feb. 2023. [Online]. Available: <https://www.energimyndigheten.se/nyhetsarkiv/2023/minskad-elanvandning-under-2022-i-sverige/>.
- [12] *Sveriges energi- och klimatmal*, Apr. 2023. [Online]. Available: <https://www.energimyndigheten.se/energiklimatmal>.
- [13] [Online]. Available: <https://energimyndigheten.a-w2m.se/FolderContents.mvc/Download?ResourceId=208766>.
- [14] K. Lundin, *Enorma vindkraftsbyggen planeras till havs*, May 2022. [Online]. Available: <https://www.di.se/hallbart-naringsliv/enorma-vindkraftsbyggen-planeras-till-havs/>.
- [15] *Roadmap 2040 - wind power: Combating climate change and improving competitiveness*<sub>2021</sub>, Jan. 2021.
- [16] 2020. [Online]. Available: [https://www.energiforetagen.se/globalassets/dokument/fardplaner/roadmap-electricity\\_swedenenergy.pdf](https://www.energiforetagen.se/globalassets/dokument/fardplaner/roadmap-electricity_swedenenergy.pdf).
- [17] [Online]. Available: <https://www.uniper.energy/sweden/about-uniper-sweden/electricity-system-future#:~:text=We%5C%20need%5C%2010%5C%20new%5C%20TWh%5C%20every%5C%20year&text=In%5C%20less%5C%20than%5C%20ten%5C%20years,industry%5C%20and%5C%20the%5C%20transportation%5C%20sector..>
- [18] V. Walter, L. Göransson, M. Taljegard, S. Öberg, and M. Odenberger, “Low-cost hydrogen in the future european electricity system – enabled by flexibility in time and space,” *Applied Energy*, vol. 330, p. 120 315, 2023. DOI: <https://doi.org/10.1016/j.apenergy.2022.120315>. [Online]. Available: <https://www.sciencedirect.com/science/article/pii/S0306261922015720>.
- [19] A. Toktarova, V. Walter, L. Göransson, and F. Johnsson, “Interaction between electrified steel production and the north european electricity system,” *Applied Energy*, vol. 310, p. 118 584, 2022. DOI: <https://doi.org/10.1016/j.apenergy.2022.118584>. [Online]. Available: <https://www.sciencedirect.com/science/article/pii/S0306261922000654>.
- [20] Svenska kraftnät, Mar. 2023. [Online]. Available: [https://www.svk.se/siteassets/om-oss/rapporter/2023/framtidens-kapacitetsmekanism-for-att-sakerstalla-resurstillracklighet-pa-elmarknaden\\_svk-2022\\_3774.pdf](https://www.svk.se/siteassets/om-oss/rapporter/2023/framtidens-kapacitetsmekanism-for-att-sakerstalla-resurstillracklighet-pa-elmarknaden_svk-2022_3774.pdf).
- [21] O. of Energy Efficiency Renewable Energy. “Wind turbines: The bigger, the better.” (2022), [Online]. Available: <https://www.energy.gov/eere/articles/wind-turbines-bigger-better>.
- [22] R. Jones, *Wind energy overview: Onshore vs offshore farm costs*, Aug. 2022. [Online]. Available: <https://www.structuresinsider.com/post/wind-energy-overview-onshore-vs-offshore-farm-costs>.

- 
- [23] *Hydrogen production: Electrolysis*. [Online]. Available: <https://www.energy.gov/eere/fuelcells/hydrogen-production-electrolysis>.
- [24] R. Cockerill, "Electrolyzer technologies. pem vs alkaline electrolysis," 2020. [Online]. Available: <https://nelhydrogen.com/wp-content/uploads/2021/07/Alk-vs-PEM.pdf>.
- [25] M. Rashid, M. Al Mesfer, H. Naseem, and M. Danish, "Hydrogen production by water electrolysis: A review of alkaline water electrolysis, pem water electrolysis and high temperature water electrolysis," *International Journal of Engineering and Advanced Technology*, vol. ISSN, pp. 2249–8958, Feb. 2015.
- [26] T. Smolinka, E. T. Ojong, and J. Garche, "Chapter 8 - hydrogen production from renewable energies—electrolyzer technologies," in *Electrochemical Energy Storage for Renewable Sources and Grid Balancing*, P. T. Moseley and J. Garche, Eds., Amsterdam: Elsevier, 2015, pp. 103–128. DOI: <https://doi.org/10.1016/B978-0-444-62616-5.00008-5>. [Online]. Available: <https://www.sciencedirect.com/science/article/pii/B9780444626165000085>.
- [27] Z. Luo, X. Wang, H. Wen, and A. Pei, "Hydrogen production from offshore wind power in south china," *International Journal of Hydrogen Energy*, vol. 47, no. 58, pp. 24 558–24 568, 2022, Hydrogen Sourced from Renewables and Clean Energy: Feasibility of Large-scale Demonstration Projects. DOI: <https://doi.org/10.1016/j.ijhydene.2022.03.162>. [Online]. Available: <https://www.sciencedirect.com/science/article/pii/S036031992201268X>.
- [28] C. Mikovits, E. Wetterlund, S. Wehrle, J. Baumgartner, and J. Schmidt, "Stronger together: Multi-annual variability of hydrogen production supported by wind power in sweden," *Applied Energy*, vol. 282, p. 116 082, 2021. DOI: <https://doi.org/10.1016/j.apenergy.2020.116082>. [Online]. Available: <https://www.sciencedirect.com/science/article/pii/S0306261920315087>.
- [29] M. R. Usman, "Hydrogen storage methods: Review and current status," *Renewable and Sustainable Energy Reviews*, vol. 167, p. 112 743, 2022. DOI: <https://doi.org/10.1016/j.rser.2022.112743>. [Online]. Available: <https://www.sciencedirect.com/science/article/pii/S1364032122006311>.
- [30] A. Małachowska, N. Łukasik, J. Mioduska, and J. Gębicki, *Hydrogen storage in geological formations-the potential of salt caverns*, Jul. 2022. [Online]. Available: <https://www.mdpi.com/1996-1073/15/14/5038>.
- [31] D. G. Caglayan *et al.*, "Technical potential of salt caverns for hydrogen storage in europe," *International Journal of Hydrogen Energy*, vol. 45, no. 11, pp. 6793–6805, 2020. DOI: <https://doi.org/10.1016/j.ijhydene.2019.12.161>. [Online]. Available: <https://www.sciencedirect.com/science/article/pii/S0360319919347299>.

- [32] [Online]. Available: <https://www.lindehydrogen.com/technology/hydrogen-storage#:~:text=For%5C%20bulk%5C%20storage%5C%20of%5C%20very,backup%5C%20for%5C%20a%5C%20pipeline%5C%20network..>
- [33] F. Johansson, J. Spross, D. R. Damasceno, J. Johansson, and H. Stille, *Investigation of research needs regarding the storage of hydrogen gas in lined rock caverns: Prestudy for Work Package 2.3 in HYBRIT Research Program 1*. Jun. 2018.
- [34] P. Forsyński, C. Oloman, S. Kazemi, T. Nickchi, and A. Usgaocar, “Development and use of a mixed-reactant fuel cell,” *Journal of Power Sources*, vol. 414, pp. 366–376, 2019. DOI: <https://doi.org/10.1016/j.jpowsour.2018.12.081>. [Online]. Available: <https://www.sciencedirect.com/science/article/pii/S0378775318314459>.
- [35] S. Öberg, M. Odenberger, and F. Johansson, “The value of flexible fuel mixing in hydrogen-fueled gas turbines – a techno-economic study,” *International Journal of Hydrogen Energy*, vol. 47, no. 74, pp. 31 684–31 702, 2022, GCGW-21 - Global Warming Reduction by Hydrogen. DOI: <https://doi.org/10.1016/j.ijhydene.2022.07.075>. [Online]. Available: <https://www.sciencedirect.com/science/article/pii/S0360319922030890>.
- [36] D. E. Agency, *Technology data - energy plants for electricity and district heating generation*, 2022.
- [37] S. Öberg, M. Odenberger, and F. Johansson, “Exploring the competitiveness of hydrogen-fueled gas turbines in future energy systems,” *International Journal of Hydrogen Energy*, vol. 47, no. 1, pp. 624–644, 2022. DOI: <https://doi.org/10.1016/j.ijhydene.2021.10.035>. [Online]. Available: <https://www.sciencedirect.com/science/article/pii/S0360319921039768>.
- [38] ETN. 2020. [Online]. Available: <https://etn.global/wp-content/uploads/2020/02/ETN-Hydrogen-Gas-Turbines-report.pdf>.
- [39] *How gas turbine power plants work*. [Online]. Available: <https://www.energy.gov/fecm/how-gas-turbine-power-plants-work>.
- [40] *Should lower-income countries build open cycle or combined cycle gas turbines?* [Online]. Available: <https://www.energyforgrowth.org/memo/should-lower-income-countries-build-open-cycle-or-combined-cycle-gas-turbines/>.
- [41] P. D. M. M. Rahman, T. Ibrahim, and A. Abdalla, “Thermodynamic performance analysis of gas turbine power plant,” *International journal of physical sciences*, vol. 6, pp. 3539–3550, Aug. 2011.
- [42] D. Jovan and G. Dolanc, “Can green hydrogen production be economically viable under current market conditions,” *Energies*, vol. 13, p. 6599, Dec. 2020. DOI: [10.3390/en13246599](https://doi.org/10.3390/en13246599).

- 
- [43] S. Öberg, M. Odenberger, and F. Johnsson, “The cost dynamics of hydrogen supply in future energy systems – a techno-economic study,” *Applied Energy*, vol. 328, p. 120233, 2022. DOI: <https://doi.org/10.1016/j.apenergy.2022.120233>. [Online]. Available: <https://www.sciencedirect.com/science/article/pii/S0306261922014908>.
- [44] Njordr, Private Communication, Apr. 2023.
- [45] *Nord pool spot glossary*, 2011.
- [46] [Online]. Available: <https://www.nordpoolgroup.com/en/trading/Operational-Message-List/2022/04/day-ahead-new-harmonised-maximum-clearing-price-from-delivery-day-wednesday-11th-may-20220411122700/>.
- [47] D. E. Agency, *Technology data - energy storage*, 2020.
- [48] D. E. Agency, *Technology data - renewable fuels*, 2022.
- [49] *Njordr offshore wind, rough\_est\_coe\_gfb.xlsx*.
- [50] [Online]. Available: <https://atb.nrel.gov/electricity/2022/index>.



# A

## Details of capacity mix Scenario 1

**Table A.1:** Details of the capacity mixes in Scenario 1: no minimum baseload with a maximum grid connection of 42%

	WF	ELY	Storage	CCGT	OCGT
Hydrogen price 2.4€/kg	5	0,61	14,41		
Hydrogen price 3€/kg	5	0,61	14,41		
Hydrogen price 4€/kg	5	0,61	14,41		

**Table A.2:** Details of the capacity mixes in Scenario 1: no minimum baseload with a maximum grid connection of 72%

	WF	ELY	Storage	CCGT	OCGT
Hydrogen price 2.4€/kg	5	0,51	9,32		
Hydrogen price 3€/kg	5	0,51	9,32		
Hydrogen price 4€/kg	5	0,51	9,32		

**Table A.3:** Details of the capacity mixes in Scenario 1: no minimum baseload with a maximum grid connection of 100%

	WF	ELY	Storage	CCGT	OCGT
Hydrogen price 2.4€/kg	5	0,43	9,24		
Hydrogen price 3€/kg	5	0,44	9,24		
Hydrogen price 4€/kg	5	0,44	9,24		



# B

## Details of capacity mix Scenario 2

**Table B.1:** Details of the capacity mixes in Scenario 2: Enforced minimum baseload with a hydrogen price of 2,4 €/kg and  $BL_{max} = 72\%$  and  $BL_{max} = 72\%$

	WF	ELY	Storage	CCGT	OCGT
BLmin 10% to 10%	5	0,83	70,52	0,50	
BLmin 10% to 15%	5	0,92	102,47	0,68	0,07
BLmin 10% to 20%	5	1,05	162,50	0,96	0,04
BLmin 15% to 15%	5	1,09	173,45	0,75	
BLmin 15% to 20%	5	1,17	206,45	0,95	0,05
BLmin 20% to 20%	5	1,54	348,83	1,00	

**Table B.2:** Details of the capacity mixes in Scenario 2: Enforced minimum baseload with a hydrogen price of 3 €/kg and  $BL_{max} = 72\%$

	WF	ELY	Storage	CCGT	OCGT
BLmin 10% to 10%	5	0,87	69,10	0,50	
BLmin 10% to 15%	5	0,97	98,45	0,68	0,07
BLmin 10% to 20%	5	1,07	158,62	0,96	0,04
BLmin 15% to 15%	5	1,11	163,21	0,75	
BLmin 15% to 20%	5	1,23	188,38	0,95	0,05
BLmin 20% to 20%	5	1,60	322,44	1,00	

**Table B.3:** Details of the capacity mixes in Scenario 2: Enforced minimum baseload with a hydrogen price of 4 €/kg and  $BL_{max} = 72\%$

	<b>WF</b>	<b>ELY</b>	<b>Storage</b>	<b>CCGT</b>	<b>OCGT</b>
<b>BLmin 10% to 10%</b>	5	0,87	69,10	0,50	
<b>BLmin 10% to 15%</b>	5	0,99	98,24	0,68	0,07
<b>BLmin 10% to 20%</b>	5	1,12	152,61	0,96	0,04
<b>BLmin 15% to 15%</b>	5	1,13	159,14	0,75	
<b>BLmin 15% to 20%</b>	5	1,29	187,43	0,95	0,05
<b>BLmin 20% to 20%</b>	5	1,70	287,04	1,00	

DEPARTMENT OF SOME SUBJECT OR TECHNOLOGY  
CHALMERS UNIVERSITY OF TECHNOLOGY  
Gothenburg, Sweden

[www.chalmers.se](http://www.chalmers.se)



**CHALMERS**  
UNIVERSITY OF TECHNOLOGY